

CHAPTER 1

INTRODUCTION

FOR millenia mankind has watched and studied the night sky. Apart from planets and comets it appeared an immutable canvas on which the stars rested. It comes as no surprise that for ancient civilizations supernovae (which were very rare events, occurring only every few centuries) were interpreted as important omens as they broke the paradigm of the unchanging night skies. As these events are so rare their origin remained a mystery until the middle of the last century. [Baade & Zwicky \(1934\)](#) suggested that "the phenomenon of a super-nova represents the transition of an ordinary star into a body of considerably smaller mass". For the last 85 years the "supernova-branch" in astronomy has been developing. There have been many advances, but there are still many unknowns. This work addresses two subfields of supernovae: The unsolved progenitor problem for Type Ia Supernovae as well as quantifying the nucleosynthetic yield and energies of Type Ia supernovae.

1.1. Ancient Supernovae

One of the earliest recorded supernovae is SN185. It first appeared in December of 185 and was visible (however fading) till the August of 187. The main record is the *Houhanshu* ([Zhao et al., 2006](#)) which had described it to be close to α Cen. Follow-up in modern times have revealed a supernova remnant in a distance of roughly 1 kpc near the α Cen ([Zhao et al., 2006](#)). SN185 is often named as the oldest written record of a supernova, this is however sometimes contested as it is still not completely clear if the so called "guest star" was a comet or a supernovae.

The oldest undisputed record of a supernova is SN1006, which also coincides with the brightest ever recorded supernova. It was observed worldwide by asian, arabic and european astronomers. [Goldstein \(1965\)](#) gives a good summary of the observations and interpretation given by these ancient observers. Ali ibn Ridwan was an Egyptian astronomer who recorded the appearance of SN1006. He wrote in a comment on Ptolemy's *Tetrabiblos*: "I will now describe for you a spectacle that I saw at the beginning of my education. This spectacle appeared in the zodiacal sign Scorpio in opposition to the sun, at which time the sun was in the 15th degree of Taurus and the spectacle in the 15th degree of Scorpio. It was a large spectacle, round in shape and its size 2.5 or 3 times the magnitude of Venus. Its light illuminated the horizon and twinkled very much. The magnitude of its brightness was a little more than a

quarter of the brightness of the moon. It continued to appear and it moved in that zodiacal sign Virgo, in setile to it, and ceased (appearing) all of a sudden. This apparition was also observed at the time by (other) scholars just as I have recorded it. "

SN1006 was later found to be a Type Ia supernova and is of significance importance in this work (see chapter ??).

[Staelin & Reifenstein \(1968\)](#) detected a pulsar in the center of SN1054. This was the first time that the stellar remnant of a supernova was found. SN1054, like SN1006, was observed by many astronomers. On of the records is a mural in the Chaco Canyon (see Figure 1.1) and was determined to have been produced around the time of the SN1054 explosion. It is still debated if SN1054 was the inspiration of the painting or the inspiration came from the passing of Hailey's comet in 1066.

SN1181 is a Galactic supernovae that has been mentioned in eight different texts by Chinese and Japanese astronomers. 3C58, a pulsar found in SN1181, is suggested as the neutron star remnant of this stellar explosion.



Figure 1.1 example caption

The supernova of 1572 has been reported by many astronomers. The most famous record, however, stems from the danish astronomer Tycho Brahe ([Brahe & Kepler, 1602](#)). The supernova was observed from November 1572 and monitored till March 1574 when it faded away from visibility. Figure 1.2 shows the original chart produced by Tycho Brahe which shows the supernova in the constellation of Cassiopeia. Nearly 400 years later [Hanbury Brown & Hazard \(1952\)](#) discovered the radio emissions from the remnant of the SN1572. SN1572 is discussed in detail in chapters ?? & ??.

Thirtytwo years after the discovery of SN1572 [Kepler \(1606\)](#) and others observed SN1604. The supernova remained visible for about 18 month. It will be discussed in this

work in chapter ?? . ??? <— This is the conclusion chapter ???

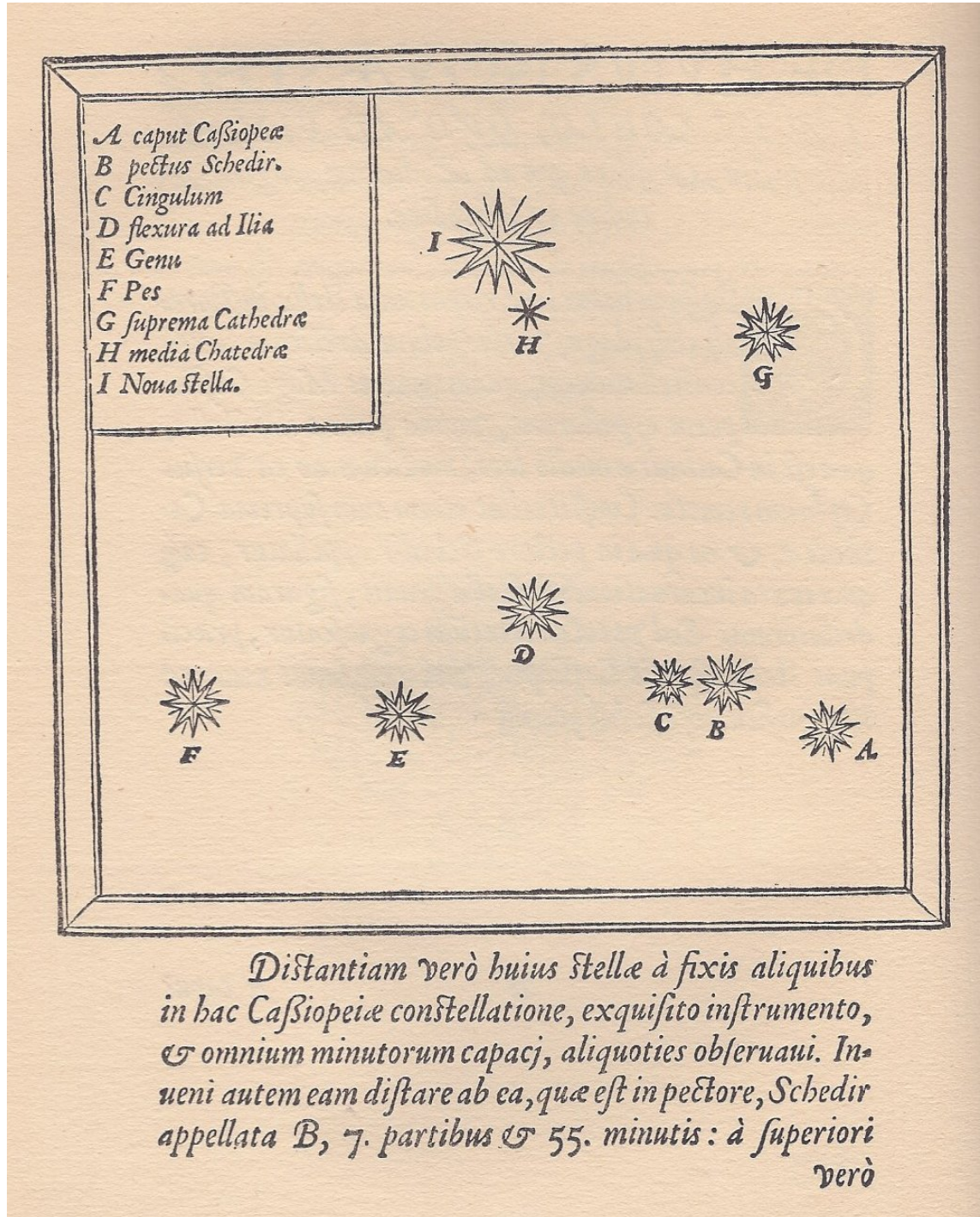


Figure 1.2 "I have indeed measured the distance of this star from some of the fixed stars in the constellation of Cassiopeia several times with an exquisit (optical) instrument, which is capable of all the fine details of measurement. I have further detected that it (the new star) is located 7 degrees and 55 minutes from the star at the breast of the Schedir designated by B." translation kindly provided by Leonhard Kretzenbacher

All of the ancient supernovae were observed only by the naked eye. Even in an era with 10-meter telescopes the records of these explosions remain useful.

1.2. Modern day supernova observations

The era of modern day supernova observations started with the discovery of SN1885. SN1885 (S Andromedae) was first spotted by Isaac Ward in Belfast in August of 1885 (Hartwig, 1885) and was visible till February 1886. More than 50 years later Baade & Zwicky (1934) coined the term supernova and established the difference between common novae and supernovae. Baade & Zwicky (1934) also suggested that these luminous events are caused by the death of stars.

In order to understand the phenomenon of the supernova better, Zwicky began a supernova search with the 18-inch Schmidt telescope. Zwicky found several supernovae which in turn inspired Minkowski to classify these supernovae by their spectra Minkowski (1941). He categorized the 14 known objects into two categories. Those without hydrogen he called 'Type I', those with hydrogen he called 'Type II' (see section 1.3.1 for a more detailed description).

With the advent of affordable computing in the 1960s the first computer controlled telescopes were build. The 24-inch telescope was built by the Northwestern University and was deployed in Corralitos Observatory in New Mexico. This search resulted in 14 supernovae.

The 1990's can be described as the decade of the supernova surveys. The Leuschner Observatory Supernova Survey began in 1992 followed shortly by the Berkeley Automatic Imaging Telescope (BAIT). These searches resulted in 15 supernovae by 1994 (van Dyk et al., 1994). One of the most well known discoveries is SN 1994D. This supernovae was observed with the Hubble Space Telescope and resulted in an image that is widely used today (see Figure ??).

These successful programmes were succeeded by the Lick Observatory Supernova Search (LOSS) using the Katzman Automatic Imaging Telescope (KAIT). By the year 2000 it had found 96 supernovae (Filippenko et al., 2001).

In addition to the search in the optical new high-energy instruments like BATSE surveyed the sky in gamma-rays. Meegan et al. (1992) that GRBs due to their isotropic distribution are events at cosmological distances rather than coming from our own Galaxy.

It was followed by the SWIFT telescope which provides, in addition to the gamma-ray-detector, an X-Ray telescope and UV/Optical telescope. It has been very successful at finding GRBs and providing targets for follow-up.

After the turn of the millenium and following the discovery of the accelerated expansion of the universe a variety of groups searched for supernovae and other transients. Some of the main contributors are the ESSENCE-collaboration,

1.3. Observational Properties of Supernovae

1.3.1. Supernova classification

The classification of supernovae started in the 1941 when Minkowski realized that there seem to be two main types (Minkowski, 1941). Those containing a hydrogen line (6563 Å) he called Type II supernovae and those showing no hydrogen he called Type I supernovae.

This basic classification has remained to this day, however the two main classes branched into several subclasses. During the 1980s the community discovered that most

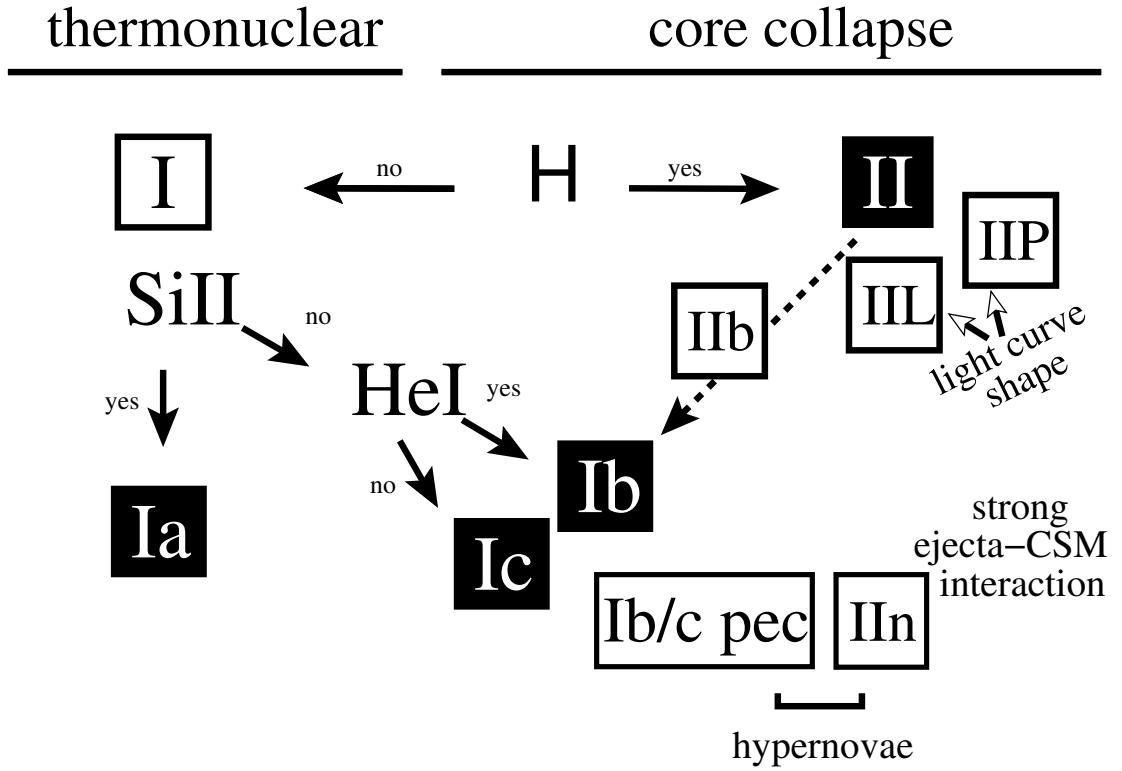


Figure 1.3

SNe Ia showed a broad Si II line at 6130 Å. There was, however, a distinct subclass of objects that lacked this feature. These Silicon-less objects were then subclassed further into objects that showed helium – now known as Type Ib – and those that did not were called Type Ic (Harkness et al., 1987; Gaskell et al., 1986). The classical Type I supernova was renamed to Type Ia (see Figure 1.3).

This classification only uses static spectral features. In recent years, however, there has been a push towards also using the lightcurve and spectral evolution as classification parameters. Benetti et al. (2005) provide an overview of this subclassing of SNe Ia and suggest that there are two distinct subclasses of SNe Ia. As a parameter for this further partitioning they use the velocity measured from the Si II feature at 6130 Å. Those with a relatively fast decline in this radial velocity they call HVG (high velocity gradient) those with a slow decline rate are named LVG (low velocity gradient). Figure 1.5 shows the velocity gradient of 26 supernovae taken from Benetti et al. (2005)

Futhermore there seems to be also a split in the intrinsic luminosity of SNe Ia. The canonical objects for these distinct brightness classes are the overluminous 1991T Phillips et al. (1992) and the faint 1991bg. Faint supernovae are fast decliners both in velocity as well as luminosity Benetti et al. (2005). The bright supernovae seem to occur in both the HVG and LVG group. I will discuss the physical implications of these two subtypes in section ??.

In summary, although there are several different subclasses the SN Ia as a class itself is relatively homogenous when compared to the different SNe II.

SNe II span large ranges in observable parameters. We can divide the main class into three main subclasses Type II Plateau Barbon et al. (SN IIP 1979) which have a relatively

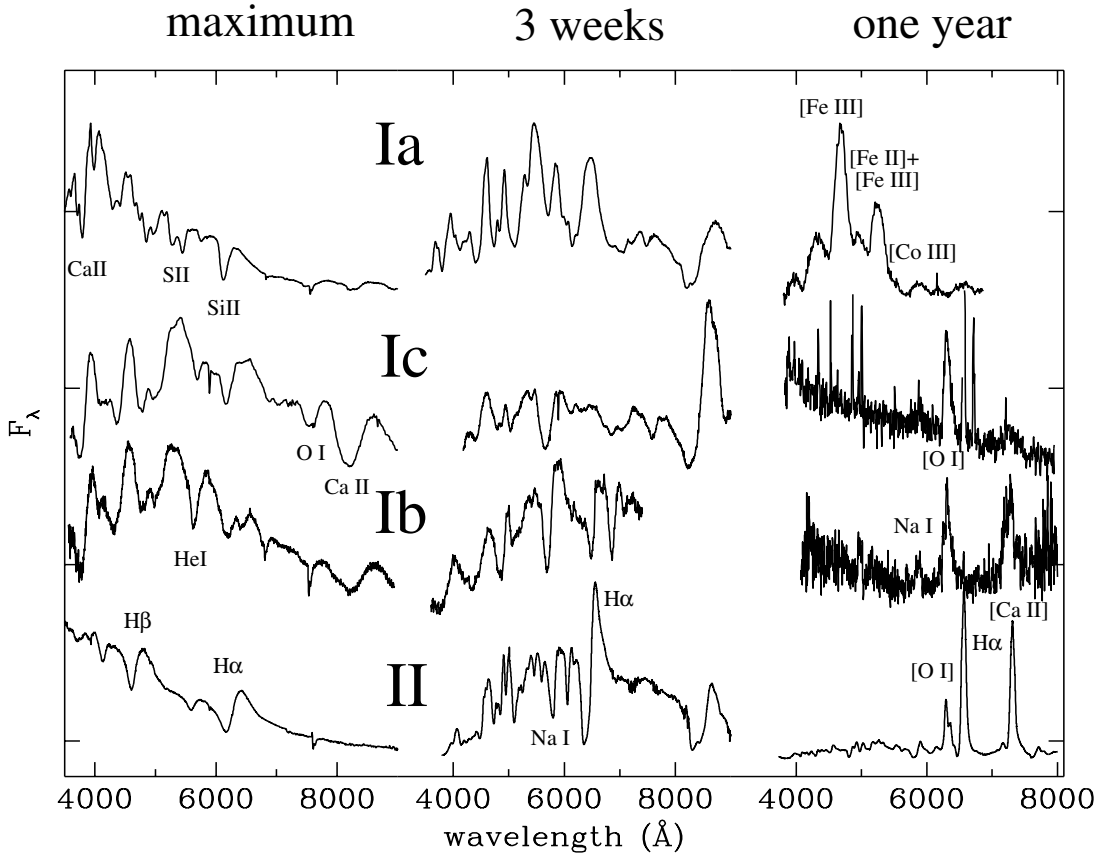


Figure 1.4 example caption

flat light curve after an initial maximum (see Figure ??), in contrast the Type II Linear (SN IIL [Schlegel, 1990](#)) has a rapid linear decline after the maximum. The third subclass is the narrow-lined SN II(SN IIn) which is characterized by narrow emission lines, which are thought to come from interaction with the CSM. Unlike the SNe Ia there are numerous intermediate objects among these three basic classes and some peculiar objects.

For a more comprehensive review of the classification of supernovae the reader should consult [Turatto \(2003\)](#); [Turatto et al. \(2007\)](#).

1.3.2. Supernova rates

The observed supernova frequency carries important information about the underlying progenitor population. In this section we will concentrate more on SNe Ia-rates but will mention SNe II and SNe Ib/c where applicable.

[Zwicky \(1938\)](#) was the first work that tried to measure the supernova rate. By monitoring a large number of fields monthly, they arrived at a supernova rate by merely dividing the number of supernova detection by the number of monitoring time and galaxies. This crude method resulted in a rate of one supernova per six centuries.

Over time many improvements were made to this first method. The rate was divided by galaxy morphological class as well as different supernova types. In addition, rates were then defined the supernova rate as number of events per century per $10^{10} L_{\odot}$ (e.g. [van den Bergh & Tammann, 1991](#); [Tammann et al., 1994](#)). In recent years, however, rate

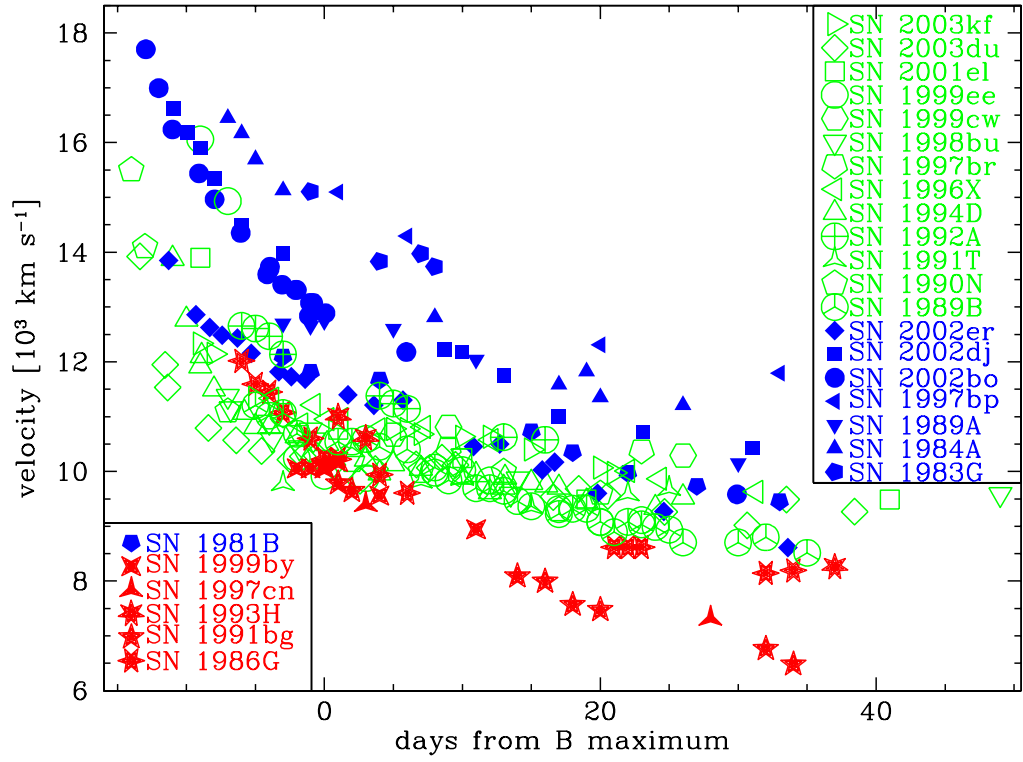


Figure 1.5 example caption

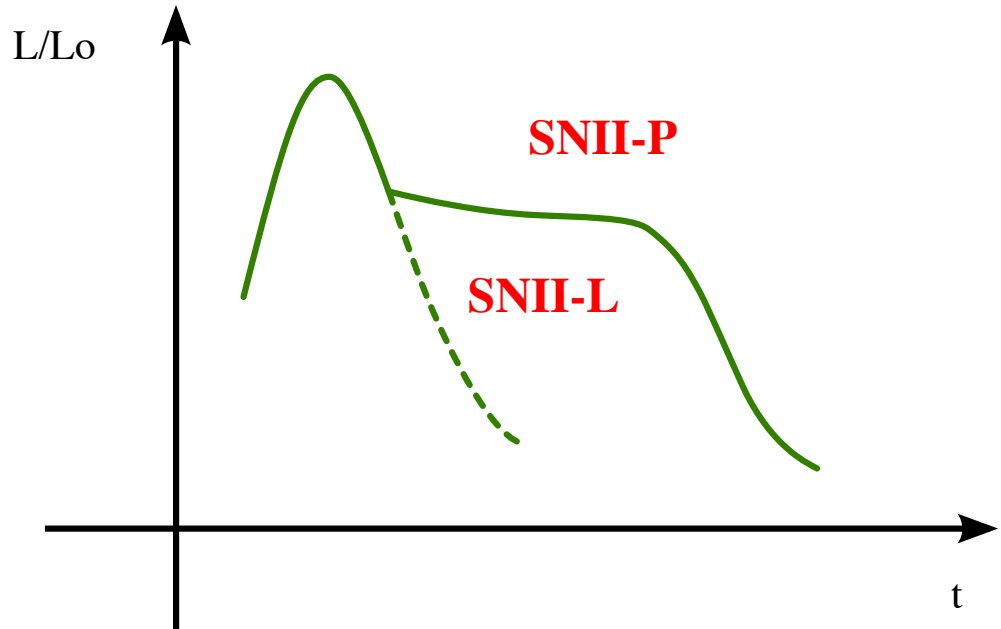


Figure 1.6 example caption

measurements is in relation to star formation rather than photometry (SN per century per $10^{10} M_{\odot}$). Therefore the community (e.g. Mannucci et al., 2005) have switched to the use of infrared photometry for the galaxy as it is thought to better represent star-formation rate than B-Band photometry (Hirashita et al., 2003).

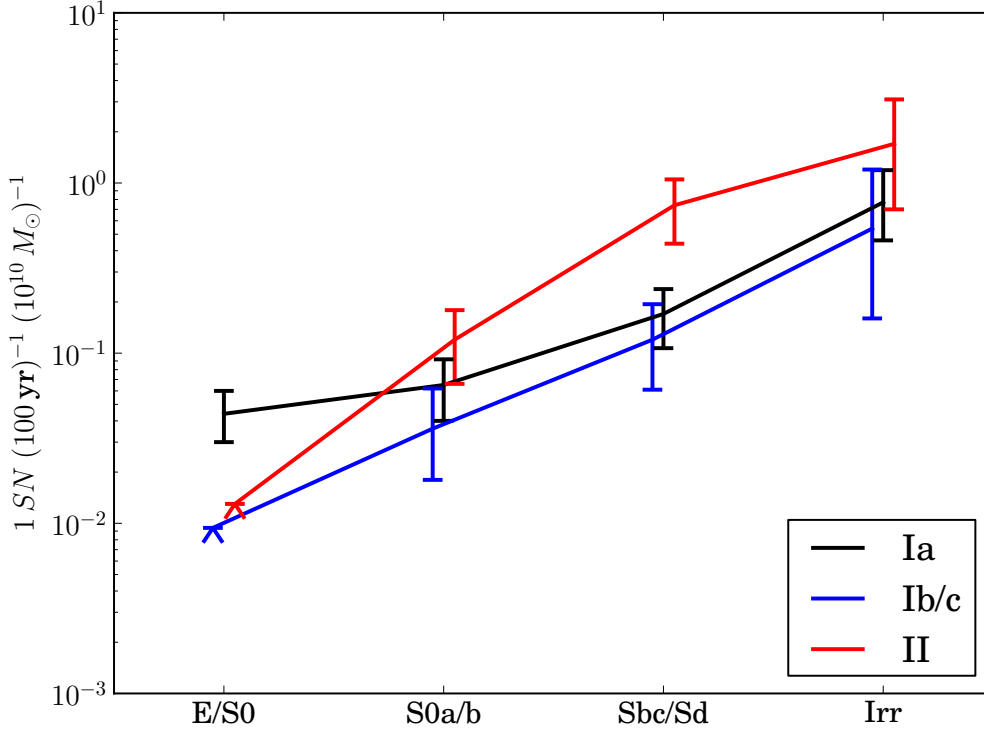


Figure 1.7 example caption

Figure 1.7 clearly shows that there is a strong connection between morphology and supernova rates. Both progenitor scenarios (single-degenerate and double-degenerate) suggest an "evolved" binary system. It is therefore puzzling that most supernovae occur in late-type spirals with a relative young stellar population. In addition, there is evidence that underluminous SNe Ia (e.g. SN 1991bg) are twice as common in late-type galaxies than in early-type galaxies (Howell, 2001). Furthermore it appears that radio-loud early-type galaxies have an enhanced rate of SNe Ia over radio-quiet galaxies (Della Valle & Panagia, 2003).

All of these factors suggest that SNe Ia can originate from two distinct progenitor scenarios and/or different explosion mechanisms (della Valle & Livio, 1994; Ruiz-Lapuente et al., 1995).

1.3.3. Light curves

Light curves were the first observables of supernovae. It contains

The light curve can be divided in four different phases (see Figure 1.8). In the first phase the SNe Ia rises to the maximum brightness. Although only a small fraction of

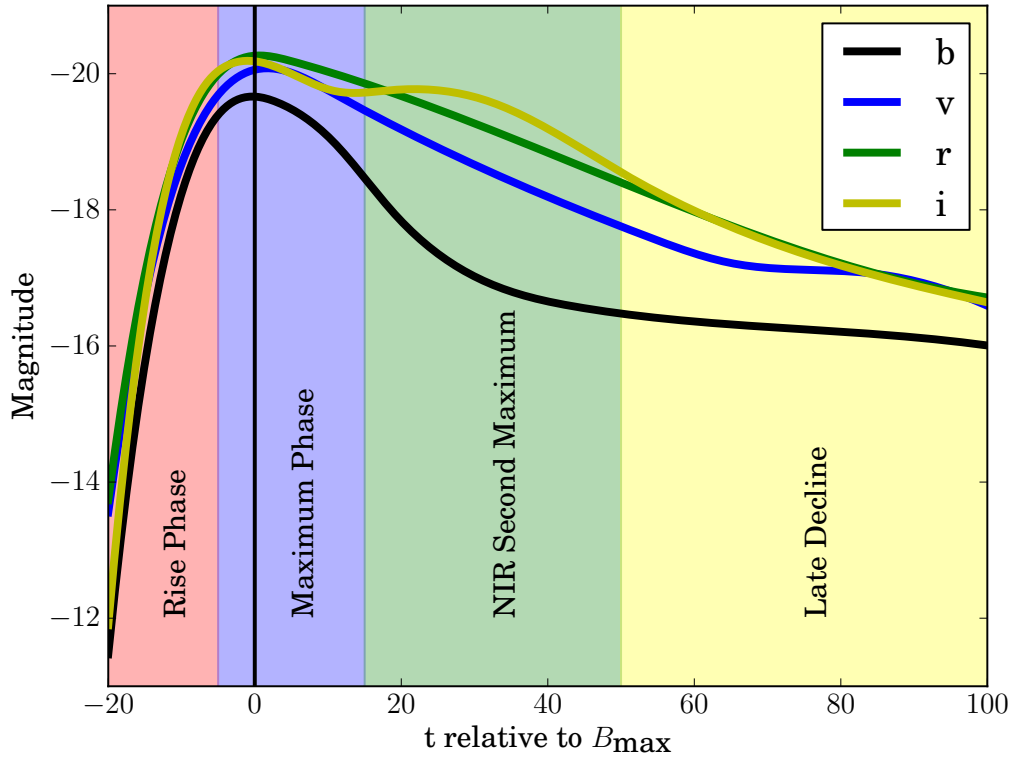


Figure 1.8 example caption

SNe Ia have been observed in that phase, one can determine the time of the explosion by approximating the very early phase of a SNe Ia with an expanding fireball. The luminosity of the fireball is

$$L \propto v^2(t + t_r)^2 T,$$

where v is the photospheric velocity, T is the temperature of the fireball, t is the time relative to the maximum and t_r is the rise time. A rise time of 19.5 days (Riess et al., 1999) seems to fit most SNe Ia.

The rise is very steep and the brightness increases by a factor of ≈ 1.5 per day until 10 days before maximum.

The SN Ia reaches the maximum first in the NIR roughly 5 days before the maximum in the B-Band (Meikle, 2000). During the pre-maximum phase the color stays fairly constant at $B-V=0.1$, but changes non-monotonically to $B-V=1.1$ 30 days after maximum.

The SN Ia starts to fade but a second maximum is observed in the NIR (Wood-Vasey et al., 2008) ??multiple citations. (Kasen, 2006) has successfully explained this by fluorescence of iron-peak elements in the NIR. See section ??.

At roughly 600 days after maximum the light curve begins ??? 1991t had a foreground dust???

Arguably the most important use of light curves is their application in normalizing SNe Ia to standard candles (see Figure ??). Phillips (1993) plotted the magnitude at maximum in different filters against the decline of the B-Band magnitude after 15 days ($\Delta m_{15}(B)$). They found a strong linear relation with a very high correlation coefficient (> 0.9). Dust

extinction in the host is one of the major systematic problems and remains so to this day.

Riess et al. (1995) refined the method by using a linear estimation algorithm. This method would deliver a distance modulus by finding the offset between a template and the supernova lightcurve. They calibrated this method against a set of SNe Ia with known distances. Light curve fitting tools are to this day in active development (e.g. Jha et al., 2007; Guy et al., 2007).

In summary, see figure x

1.3.4. Spectra

Spectra are much more detailed measurements of Supernovae. They are however, observationally much more expensive.

Supernovae spectra can be divided in two phases: the photospheric phase and the nebular phase. In the photospheric phase, the spectrum can be very well approximated by a dense optically thick core which has a black-body radiating surface. Above this photosphere is an optically thin ejecta wind. Photons are usually not created in the optically thin ejecta. The ejecta rather reprocesses the radiation field coming from the photosphere. In the case of SNe Ia the core consists mainly of decaying ^{56}Ni which produces the energy for the radiating photosphere. For SNe II the core consists mainly of ionized hydrogen.

As the supernova expands the photosphere recedes further into the core and the optically thin layer grows larger and larger. Once sufficiently expanded the entire SN ejecta becomes optically thin. This phase is dominated by strong emission peaks and no continuum.

SNe Ia spectra

SNe Ia spectra span many different applications, but foremost they help us to understand the physical processes in the thermonuclear explosion. Shortly after the explosion the ejecta is in homologous expansion. The observed spectra are characterized by an underlying continuum - emitted from the photosphere - and absorption features from the ejecta material above the photosphere. As time passes the photosphere recedes into the remnant and deeper layers of the exploded white dwarf become spectroscopically visible. Synthetic modelling of spectra is an important component to understanding SNe Ia and will be discussed in detail in Chapter ??.

This time-variability in the spectra is used to conduct tomography on SNe Ia (Stehle et al., 2005).

Similar to light-curves the spectra have different phases. We will use the "normal"-SN Ia SN 2003du to demonstrate the spectral evolution (Tanaka et al., 2011).

Pre-Maximum Phase In the pre-maximum phase the spectrum shows very high velocities (up to $18\,000\text{ km s}^{-1}$). There is a relatively well defined pseudo-continuum with strong P Cygni-profiles of IMEs and iron-group elements (see Figure ??). These iron-group elements are primordial as the burning in the outer layers (visible at these early times) is incomplete and does not produce these elements.

The Ca Roman2 line is very prominent in the blue and often shows extremely high velocities at early times (in SN 2003du $v\,25000\text{ km s}^{-1}$). There have been multiple suggestion for the cause of this unusual velocity, including interaction with Calcium in the ISM or

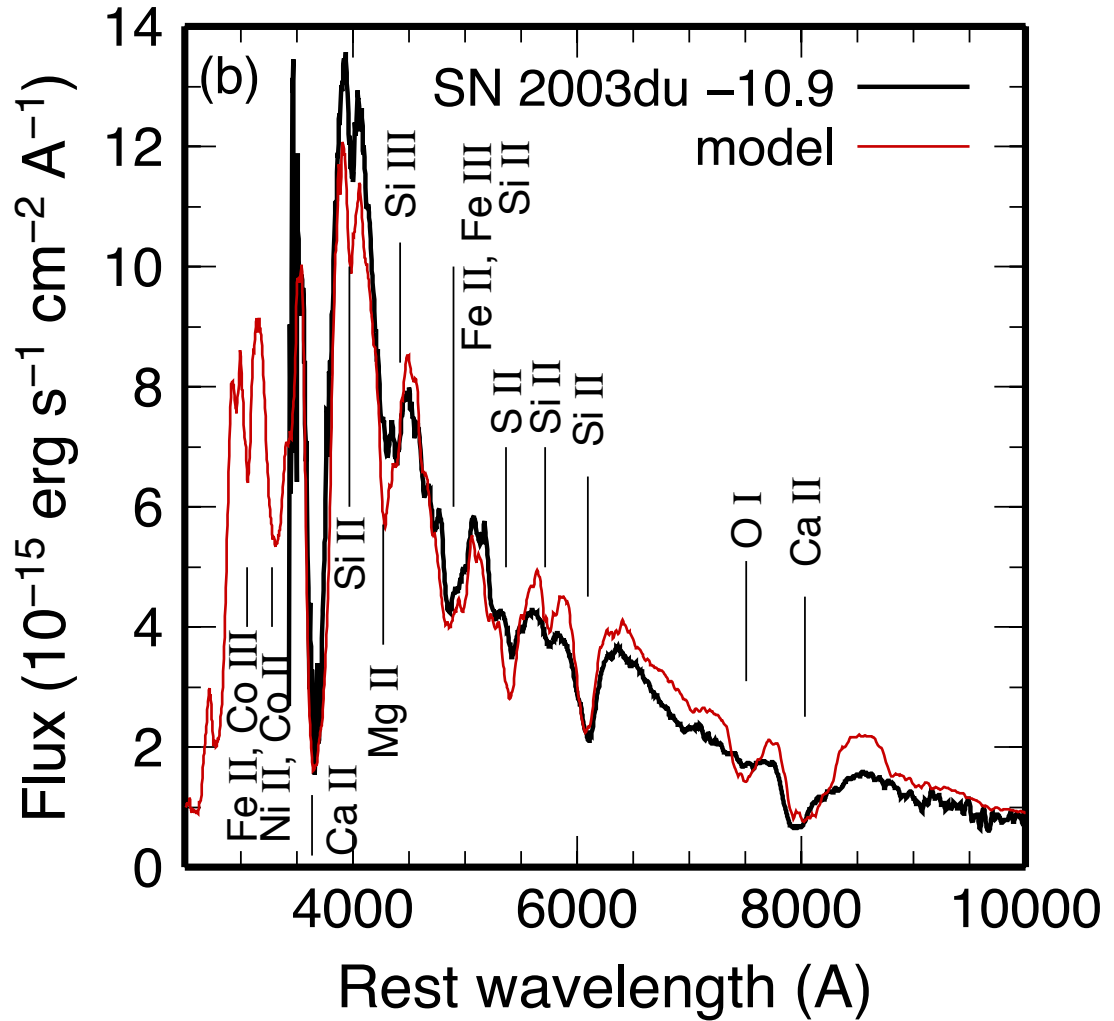


Figure 1.9 example caption

high-velocity ejecta blobs (Hatano et al., 1999; Gerardy et al., 2004; Thomas et al., 2004; Mazzali et al., 2005; Quimby et al., 2006; Tanaka et al., 2006; Garavini et al., 2007). There is a strong Mg Roman2 feature at 4200 Å which is contaminated by several iron lines. Silicon and Sulphur both have strong features 5640 Å (S Roman2) and at 6355 Å (Si Roman2). The strong Silicon feature distinguishes SNe Ia against other supernovae in the Type I-group.

It is believed that in these early phases one should be able to see Carbon and Oxygen from the unburned outer layers. There is the C Roman2-feature at 6578 Å but it is normally very weak (if visible at all). The Oxygen triple feature at 7774 Å is seldom very strong. ??? ask stephan ??

Maximum Phase As the supernova rises to the peak luminosity a large fraction of iron group elements (especially ^{56}Ni) is suppressing flux in the UV and reemitting it in the optical (see Figure 1.10). The silicon lines become narrower (??only in 03du??) as the photosphere reaches material deeper in the remnant. The ratio of the Silicon lines Si Roman2 5972 Å and Si Roman2 6355 Å is a good indicator for temperature (Nugent et al., 1995).

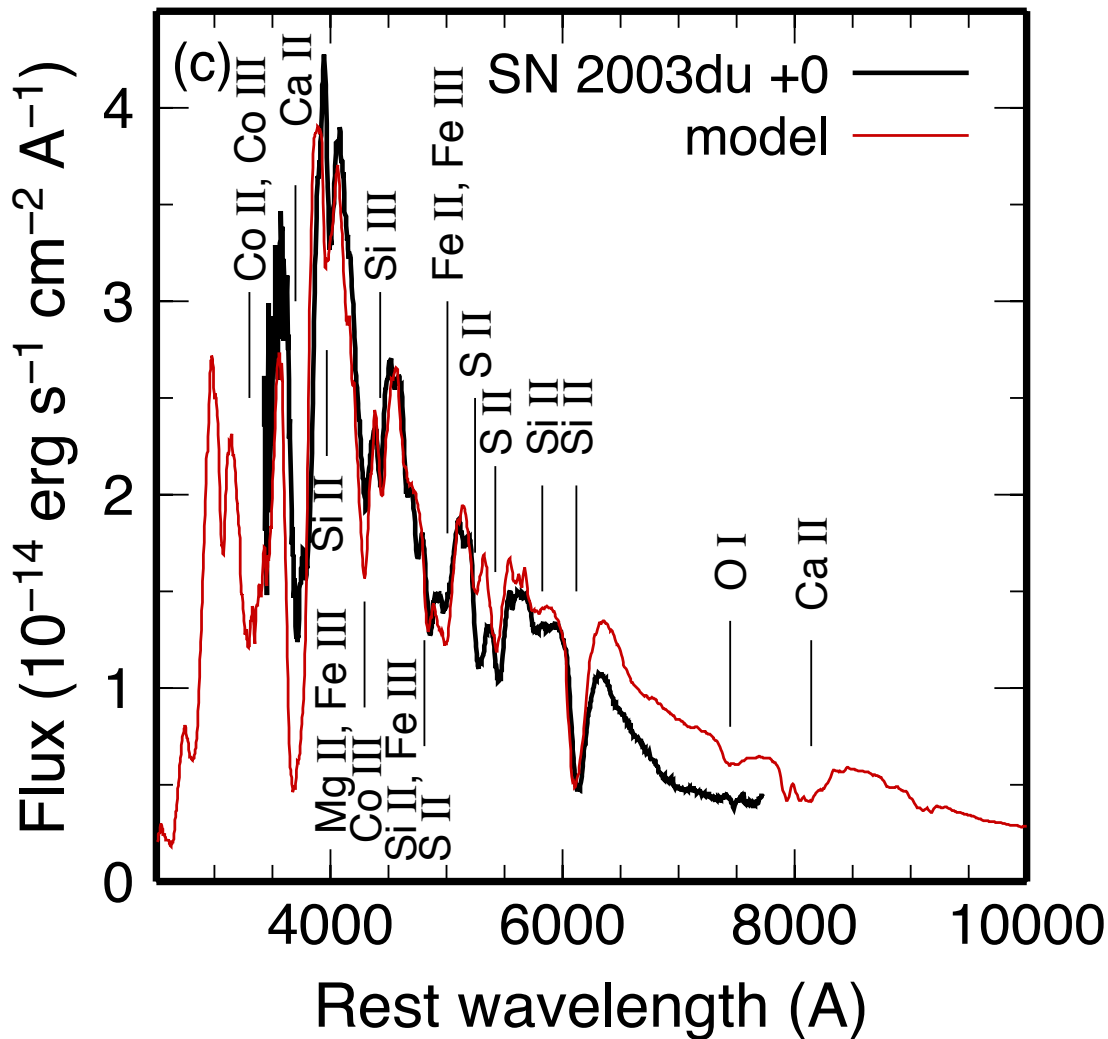


Figure 1.10 example caption

Post-Maximum phase The contribution from iron-group elements is still rising, while the photospheric velocity has decreased to less than 10000 km s^{-1} (see Figure 1.11). The strong Calcium feature at 4000 \AA is disappearing.

Nebular-Phase As the supernova fades, the photosphere disappears. At this stage the spectrum is now characterized by strong emission lines which are produced by the elements from the very core of the explosion (see Figure 1.12). The velocity has fallen under 5000 km s^{-1} (??check??).

SNe II Spectra

SNe II show much more variation in their spectra for each object than SNe Ia. In this section we will only give a very general and brief overview over SNe II spectra and spectral evolution. Compared to SNe Ia the initial spectrum is a relatively undisturbed continuum (see 1.4). The only strong lines visible are those of Hydrogen and Helium which are the

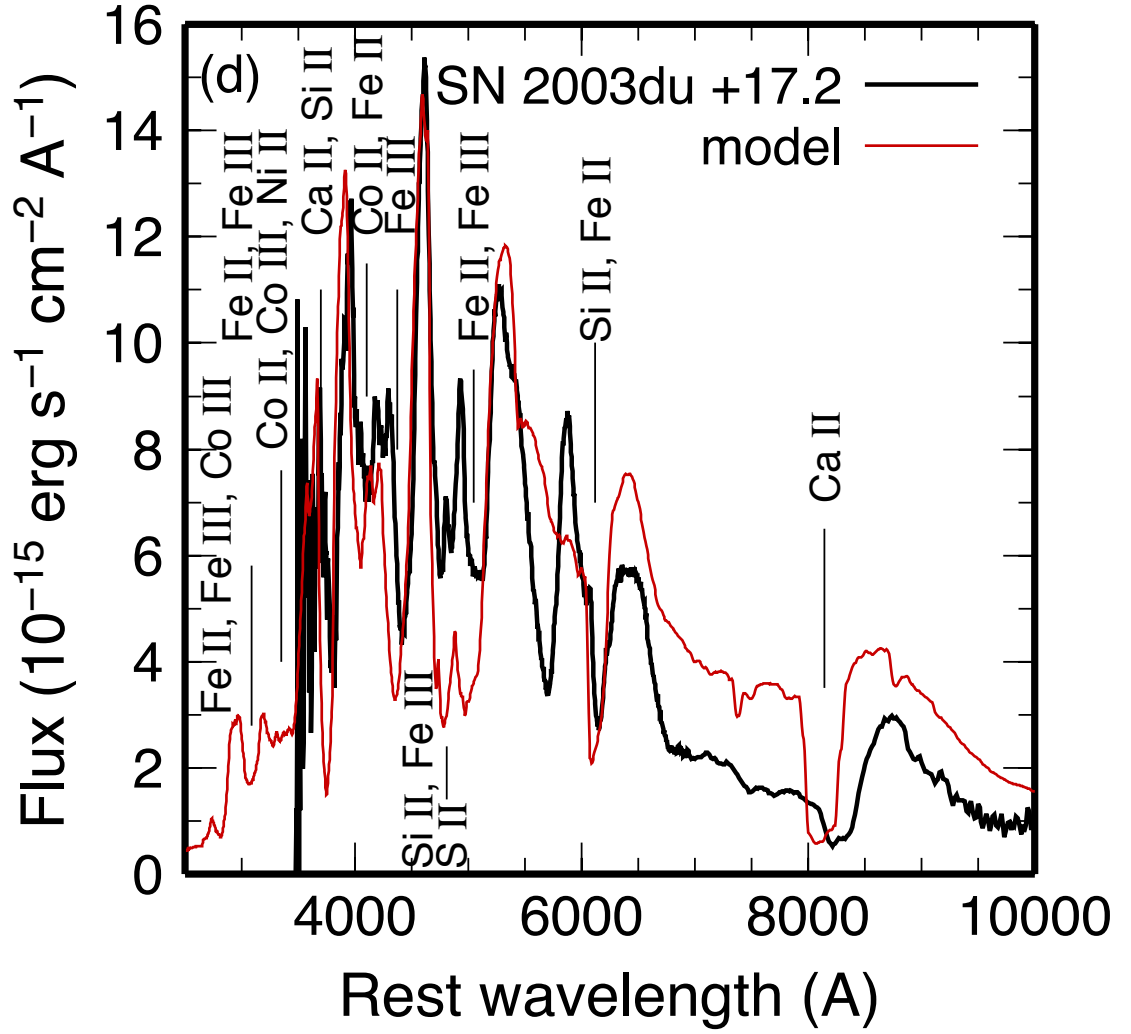


Figure 1.11 example caption

elements present in the envelopes of the progenitors. As the photosphere recedes into the core heavier elements like Oxygen, Magnesium and Iron become visible.

The nebular spectra are characterized by $H\alpha$, Oxygen and Calcium emission lines.

1.3.5. X-Ray & Radio observations

Compared to the traditional optical astronomy X-Ray & Radio are relatively new fields. The information carried in the very high and low frequency photons is invaluable to understanding various transient events.

X-Ray & Radio observations in the case of SNe Ia can for example reveal the shock interaction of the ejecta with the CSM. The single degenerate scenario predicts much more CSM than the double degenerate scenario. X-Ray ([Hughes et al., 2007](#)) and Radio Observations ([Hancock et al., 2011](#)) have however not revealed any emission in either Band. This could hint that the double degenerate scenario is the more common, but many caveats remain.

The long GRB-phenomenon has been suggested to be the relativistic jet launched in

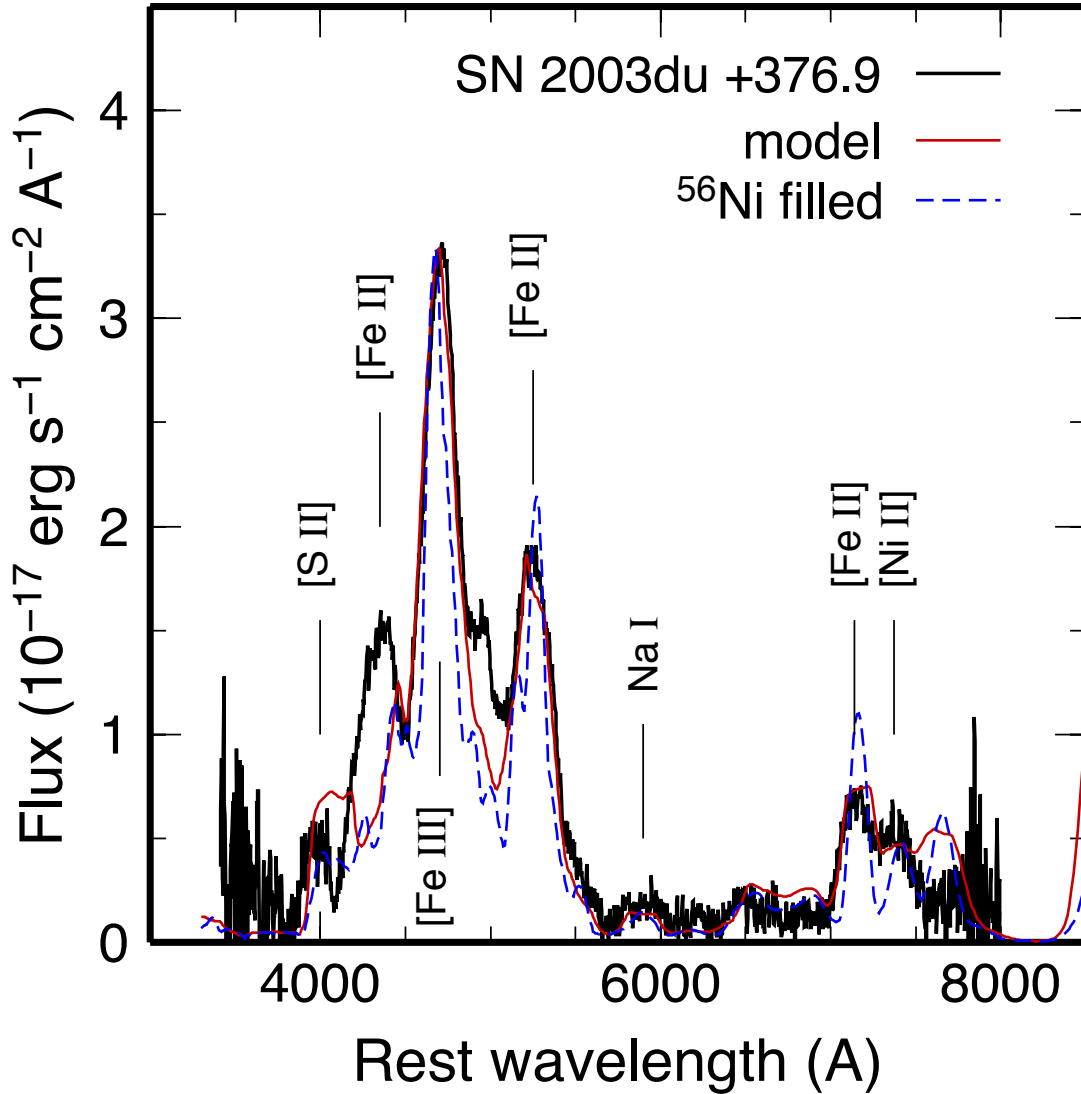


Figure 1.12 example caption

a SN Ib/c. In their late phase GRB's jet spreads and is thought to emit isotropically in radio. This radio glow should be visible to both on-axis and off-axis observers, but has so far only been observed on-axis. [Soderberg et al. \(2006\)](#) have tried to find this isotropic radio emission at late times on SN Ib/c to see if they are off-axis GRBs. The study however remained inconclusive.

SNe II have long been theorized to emit X-Rays at shock breakout ([Klein & Chevalier, 1978](#); ?). To observe them is technically very challenging as the supernova needs to be detected very early on. SN2008D was serendipitously discovered as the Swift X-Ray telescope picked up an extremely luminous source. Subsequent ground based follow-up revealed a brightening optical counterpart.

Radio and X-Ray observation of both kinds of supernovae are still in its infancy and will provide great help when solving the current mysteries surrounding all types of supernovae.

1.3.6. Supernova Cosmology

Early in the last century astronomers were trying to gauge our place in the universe. The question of distances to several astronomical objects arose. A distance probe is an astronomical phenomenon. Over time many distance-independent luminosity relations were discovered such as the absolute Magnitude-Period relation of Cepheids. The discovery of these standard candles led to the creation of the field of cosmology.

Supernovae have played a vital role in discovering the current structure of the Universe

SN II Cosmology: SN IIP have been first suggested as cosmological probes by [Kirshner & Kwan \(1974\)](#). It is important for cosmological distance probes to know the intrinsic luminosity precisely. At the plateau-phase of the supernova, caused by the hydrogen-recombination, the temperature is well known ($T=5000$ K). In addition it is assumed that the supernova is in free expansion, thus a measurement of the velocity and an assumption of the initial radius results in a known radius. Assuming the supernova to be a blackbody during plateau-phase one can then calculate a luminosity using the radius and the temperature. SN IIP as distance candles, however, are observationally expensive and not as accurate as SN Ia as standard candles (15% error for SN II ([Nugent et al., 2006](#)) vs 7% error for SN Ia).

SN Ia Cosmology SNe Ia have been one of the most successful distance probes. It is believed that SNe Ia are the explosion of C-O white dwarfs. The brightness of these objects is powered by the decay of ^{56}Ni . The quantity of ^{56}Ni produced in the explosion can be gauged from the evolution of the light-curve which then in turn can be used to calibrate the intrinsic brightness (see Figure 1.13). In the late 1990s new detector technologies (CCDs), computing and new telescopes made it possible to measure the lightcurves of many SNe Ia accurately.

[Hubble \(1929\)](#) made the discovery that more distant galaxies move at higher velocities. It was implied that the universe is in a state of constant expansion. The amazing discovery that both [Riess et al. \(1998\)](#) and [Perlmutter et al. \(1999\)](#) made with SNe Ia was that the universe, in stark contrast to the earlier assumption, was expanding at an accelerating rate.

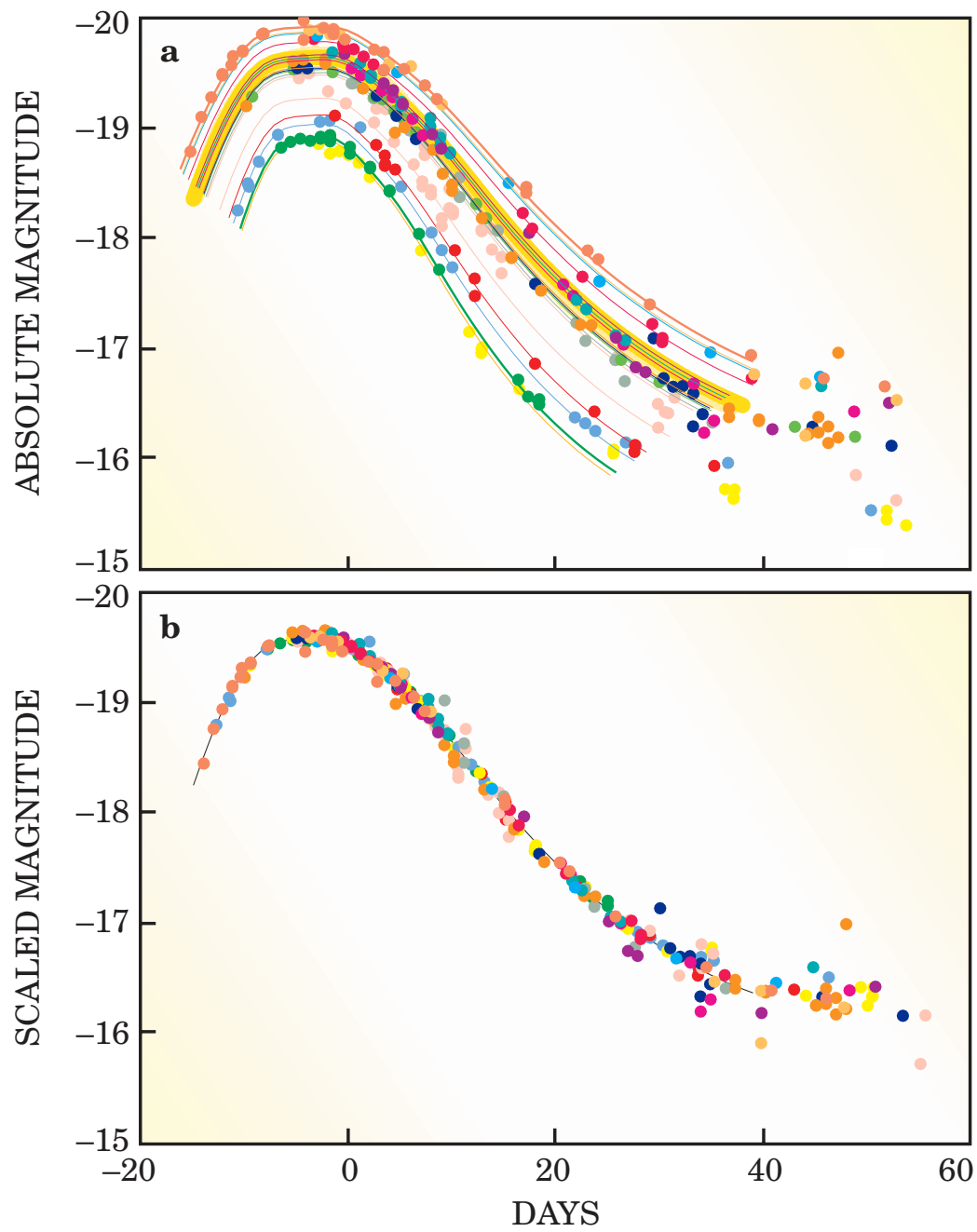


Figure 1.13 Replace with Brad data

1.4. Core-Collapse Supernova Theory

All SN II are believed to be powered by the collapse of the electron-degenerate iron core of massive stars. For the iron core to form there had to be several prior stages of evolution.

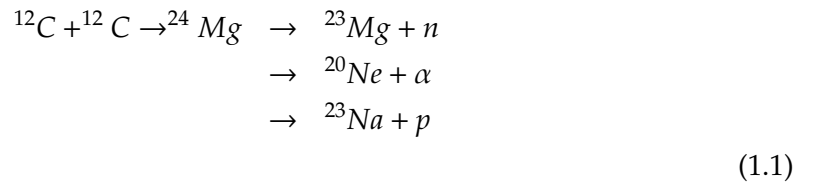
1.4.1. Evolution of Massive Stars:

To understand the state of the star shortly before supernova evolution it is imperative to follow its evolution. For the topic of SN II we will concentrate on the nuclear physics of massive star evolution in this section. In the scope of this work we will follow a single massive star as a progenitor. There has been ample suggestions that some SN II progenitors are binary, but their evolution is much more complex and is outside the scope of this work?? citation needed??. In this context massive stars are stars bigger than $8 M_{\odot}$. This is the minimum mass for a star that is believed to explode in a SN II. Like all stars massive stars spend most of their lives on the main-sequence burning hydrogen. This happens via the carbon-nitrogen-oxygen cycle and its various side-channels (e.g $^{12}\text{C}(p, \gamma) \rightarrow ^{13}\text{N}(e^+\nu) \rightarrow ^{13}\text{C}(p, \gamma) \rightarrow ^{14}\text{N}(p, \gamma) \rightarrow ^{15}\text{O}(e^+\nu) \rightarrow ^{15}\text{N}(p, \alpha) \rightarrow ^{12}\text{C}$). For a $20 M_{\odot}$ star this phase lasts for 8.13 Myr (see [Woosley et al. \(2002\)](#)).

As the star evolves it begins to ignite Helium which burns via the triple- α process to Carbon ($3\alpha \rightarrow ^{12}\text{C}$) and then to Oxygen ($^{12}\text{C}(\alpha, \gamma) \rightarrow ^{16}\text{O}$). Table 1 in [Woosley et al. \(2002\)](#) lists 1.17 Myr for this phase.

Due to neutrino losses the stellar evolution is qualitatively different after helium burning. A neutrino-mediated Kelvin-Helmholtz contraction of the carbon-oxygen core describes the advanced stages of nuclear burning in massive stars well ([Woosley et al. \(2002\)](#)). This contraction is occasionally delayed when the burning of new fuel sources counteracts the neutrino losses. The star in the end is composited of a series of shells that burn the above fuel and deposit the ashes on the shell below (see Figure 1.14). There are four distinct burning stages. Their principal fuels are carbon, neon, oxygen, magnesium and silicon.

In the carbon burning stage two ^{12}C nuclei are fused to an excited state of Magnesium which then decays slowly to ^{23}Na (see 1.2).



Although oxygen has a lower Coulomb barrier, the next nucleus to burn after Carbon is Neon. This layer is composed of ^{16}O , ^{20}Ne and ^{24}Mg and burns Neon with high-energy photons from the tail of the Planck distribution ($^{20}\text{Ne}(\gamma, \alpha)^{16}\text{O}$).

In the next shell there is a composition of mainly ^{16}O , ^{24}Mg and ^{28}Si . The bulk nucleosynthetic reaction is shown in 1.2.

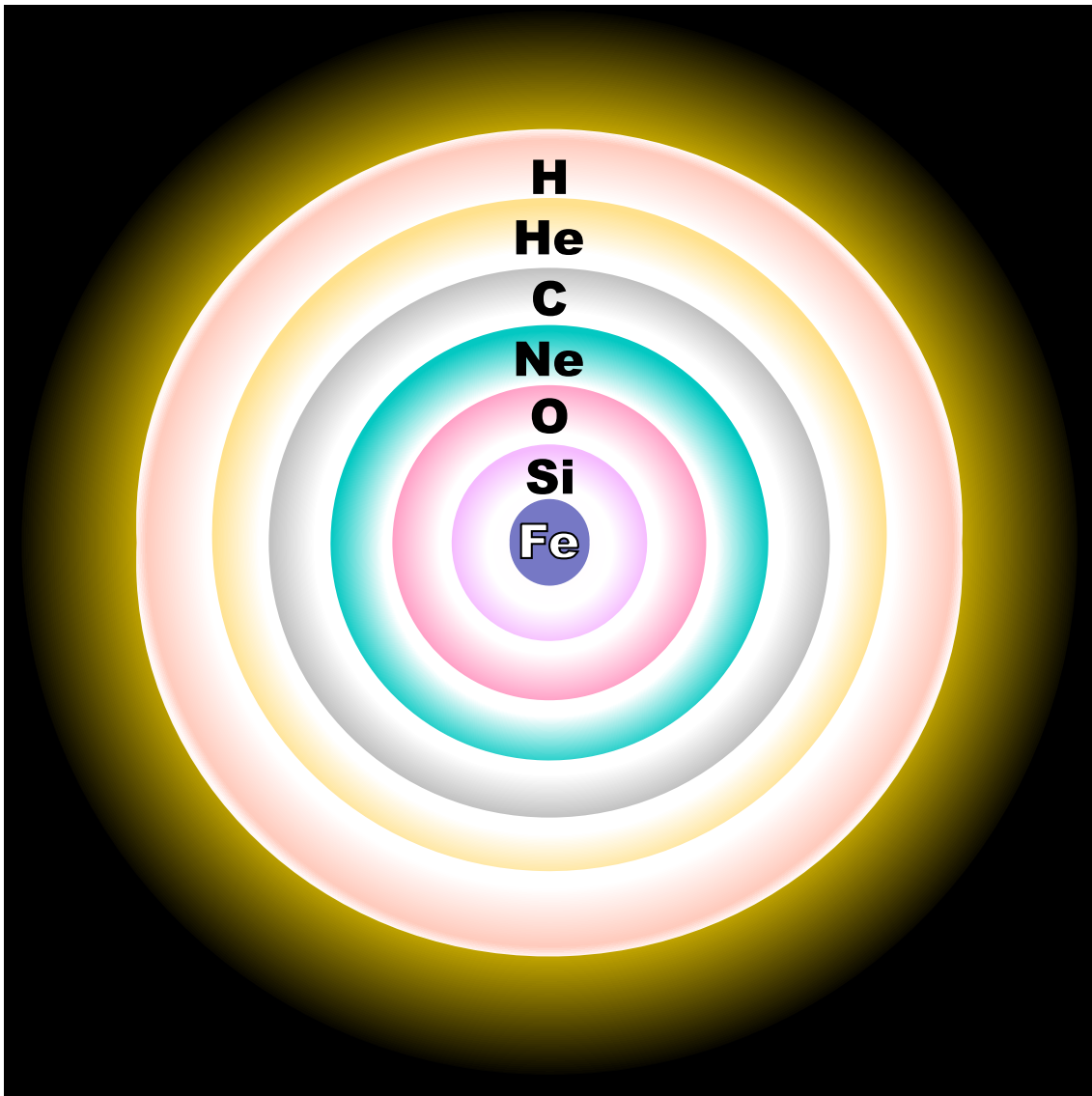
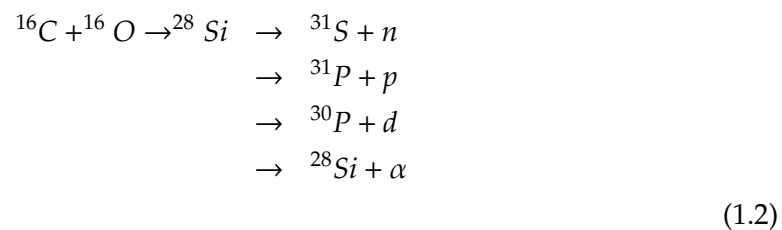


Figure 1.14 example caption



The last shell is of burning ${}^{28}\text{Si}$ to ${}^{56}\text{Ni}$ is very complex. The obvious reaction ${}^{28}\text{Si} + {}^{28}\text{Si} \rightarrow {}^{56}\text{Ni}$ does not take place, but is replaced by a very complex network of isotopes to burn to ${}^{56}\text{Ni}$. In simulations this is computationally intensive and numerically unstable (e.g . [Weaver et al. \(1978\)](#) who carry a 128-isotope network). Following silicon burning the composition consists of mainly iron-group nuclei. At the end of silicon burning we are reaching nuclear statistical equilibrium.

1.4.2. Core collapse

Before the collapse the core, consisting of iron peak elements. Neutrino losses during carbon and oxygen burning decreased the central entropy sufficiently so that the core becomes electron degenerate. Such a degenerate core, which is higher than the Chandrasekhar mass (adjusted for Y_e , entropy, boundary pressure and other parameters will collapse.

There are two main instabilities that facilitate the collapse. As the density rises the Fermi-Energy becomes high enough for electrons to capture onto iron-group nuclei. This capture process removes electrons that were providing degeneracy pressure and reduces the structural adiabatic index.

The second instability is the rise to temperatures where the nuclear statistical equilibrium favours free α -particles. The collapse eventually leads to nuclear densities, the hard-core potential acts as a stiff spring during the compressive phase. It stores up energy and eventually releases this energy resulting in a "core bounce". [Baron et al. \(1985, 1987\)](#) believed the core bounce to provide the energy for the ensuing supernova explosion. More recent simulations however show that the bounce shock is not sufficient for a SN II explosion. The bounce shock loses energy by photo disintegrating the nuclei it encounters (losing roughly 10^{51} erg per $0.1 M_\odot$). Different neutrino flavours that the resulting neutrino winds likely play a big role.

The energy for a successful explosion is now thought to come from neutrino energy deposition. This reinvigorates the shock and leads eventually to an explosion which ejects the envelope of the massive star. A newly born neutron star is left behind.

The precise explosion mechanism is unknown. Using progenitor models with different parameters like rotation and mass lead to different outcomes. [Woosley et al. \(2002\)](#) provide a very comprehensive review of the theory of evolution and core collapse. In particular they lay out a more extensive description of the scenarios after core-bounce.

1.4.3. Pair instability

One explosion scenario is the pair-instability supernova. This scenario is believed to only happen in stars with a helium core of more than $40 M_\odot$. After core helium burning the star starts to contract at an accelerated rate. The energy released during this process is used to produce electron-positron pairs rather than raising the temperature. If significant densities are reached, oxygen fusion eventually halts the implosion and the collapse bounces to an explosion. For very high stellar masses it is believed that oxygen fusion does not provide enough energy to halt the contraction and the star collapses to a black hole.

1.4.4. Type II Supernovae

The observables of these stellar cataclysm are the light curve, spectra and for one case even the neutrino wind. The supernovae goes through three distinct phases which can be observed.

The shock-breakout is the first visible signal from the supernova. [Ensman & Burrows \(1992\)](#) calculated a duration for the shock breakout of SN1987A to 180 s three minutes, its luminosity of $5 \times 10^{44} \text{ erg s}^{-1}$. Thus far it has been observed only once in 2008D ([Soderberg et al., 2008](#)). They report a duration of 400 s with a luminosity of $6.1 \times 10^{43} \text{ erg s}^{-1}$.

The plateau seen in many SN II (see figure 1.6) is produced by the recombination of hydrogen when hydrogen-rich zones cool to less than 5500 K. The radiation comes effect-

ively from a blackbody, whose luminosity is determined by the radius of the photosphere. Supernovae of Type III do not show this behaviour and are thus thought to have no or a very small hydrogen envelope.

After the recombination of hydrogen the light-curve drops off linearly and we see radioactivity providing the main energy source. ^{56}Ni decays to ^{56}Co with a half-life of 6.1 d and then further to ^{56}Fe with a half-life of 77 d. Most of the energy of the ^{56}Ni decay is used to accelerate the expansion of the core. The tail of the light-curve after the plateau is mainly powered by the decay of ^{56}Co . Some light can also be produced by shock interaction with the CSM.

1.4.5. Type Ib/c supernovae

If the star lost all of its hydrogen envelope prior to core-collapse there is no plateau visible in the light-curve. Instead the light-curve is powered by radio-active decay after shock breakout. In addition, the hydrogen lines are not visible in the spectrum. This leads to the supernova being classified as Type I. If both hydrogen and helium envelopes are lost then the supernova is classified as Type Ic. This loss of envelope is presumed to be caused by stellar winds or binary interactions (citation needed).

1.4.6. Gamma Ray Burst

1.5. Thermonuclear Supernova Theory

In this section we will discuss the theory of SNe Ia. We will, however, focus mainly on the explosion mechanism and not the theoretical implications of different progenitor scenarios. As this work is focussing considerably on SN Ia-progenitors we will dedicate a section on the different progenitor models (see 1.6).

1.5.1. White Dwarfs

White dwarfs are thought to be the progenitor stars of Type Ia supernovae. These objects are among the few that do not have hydrogen, which would explain the lack of hydrogen in SN Ia-spectra. It is generally believed in the community that these objects accrete matter (for the possible scenarios see section 1.6) until they get close to the Chandrasekhar-mass (Chandrasekhar, 1931). It is a delicate balance between the ignition point that results in the thermonuclear run-away and the Chandrasekhar threshold which leads to a collapse of the star to a neutron star.

There are three main classes of white dwarfs: Helium, Carbon/Oxygen (henceforth CO-WD) and Oxygen/Neon/Magnesium (henceforth ONe-WD) white dwarfs. Helium white dwarfs would start burning their Helium to Carbon and Oxygen well before it gets near the Chandrasekhar mass. In addition, these objects can also be ruled out as progenitors for SNe Ia as copious amounts of IGE produced in SNe Ia which are not consistent with the burning of a Helium white dwarf.

The ultimate fate of a ONe-WD is thought to be the collapse into a neutron star. Once the ONe-WD is heavy enough electron capture begins in the core ($^{20}\text{Ne}(e^-, \nu)^{20}\text{F}(e^-, \nu)^{20}\text{O}$). Heating by the resulting γ -rays starts explosive Oxygen burning. However, the electron-capture is much faster than the Oxygen burning and promotes the collapse to a neutron star (Nomoto & Kondo, 1991; Gutiérrez et al., 2005).

The favoured progenitor for a SN Ia are CO-WDs. Most of these objects are born, however, with a mass around $0.6 M_{\odot}$ (Kepler et al., 2007). It is thought that they accrete mass until they are getting close to the Chandrasekhar mass and then explode as a SN Ia.

1.5.2. Pre-supernova evolution

The white dwarf gradually accretes more and more material. At some instant mild carbon burning ensues



, but is mediated by photon and neutrino losses (Lesaffre et al., 2005; Iliadis, 2007). As the cooling processes become less effective convection starts in the core. The energy output in the core increases. At this stage the thermal structure is largely controlled by Urca pairs. These reaction pairs consist of alternating electron captures and β^- -decays involving the same pair of parent and daughter nuclei. Two prominent examples which are important in pre-supernova evolution are ${}^{21}\text{Ne}/{}^{21}\text{F}$:



These processes can lead to either cooling or heating. Lesaffre et al. (2005) have modelled this process in a convective core.

Ultimately, the pre-supernova evolution is hard to model theoretically as it is likely to be nonlocal, time-dependent, three dimensional and stretches over very long timescale. The exact conditions at the time of explosion are therefore unknown. All explosion models have to assume simple initial conditions.

Ignition The Urca processes will dominate core evolution for the last thousand years until explosion. As the temperature rises to $T \approx 7 \times 10^8 \text{ K}$ (Hillebrandt & Niemeyer, 2000) the convection time (τ_c) increases and becomes comparable to the burning time (τ_b). Consequently the convective plumes burn as they circulate. Once the temperature reaches $T \approx 10^9 \text{ K}$ τ_b becomes very small compared to τ_c and Carbon and Oxygen essentially burn in place. This is the moment of ignition. As the convective plumes burn while they rise it is likely that the initial flame seed does not start in the center of the core. Röpke & Hillebrandt (2005) have used multiple flame seeds in their three dimensional full star models.

Thermonuclear Explosion From this point, initially there were two main options. The first option was the complete detonation (supersonic flame front) of the CO-WD (Arnett, 1969). It was quickly discovered, however that this method burns to NSE and thus produces no IME. These IME are observed in SN Ia.

For a long time it was then suspected that the star instead of detonating would deflagrate (subsonic flame wave, mediated by thermal conduction). The fuel in front of the deflagration gets rarified by the energy from the flame. Hot light burning bubbles rise into the cold dense fuel and create Rayleigh-Taylor instabilities (see Figure 1.15 at $t=0.72 \text{ s}$).

Once the deflagration wave has run through the star, the resulting production of ^{56}Ni is not enough to explain the light curve of normal SN Ia. The deflagration produces roughly $0.3 M_{\odot}$ of ^{56}Ni , to power the light curve of normal SNe Ia one needs $0.6 M_{\odot}$ (Mazzali et al., 2007).

The currently favored scenario is the one of delayed detonation. The star initially burns like in the deflagration scenario, then inhomogeneities in the deflagration front produce hotspots. In these hotspots the temperature gradients are so high that detonation waves form. The ensuing detonation front can only burn the cold unburnt-fuel and does not penetrate the ashes of the deflagration. Figure 1.15 shows clearly how the detonation wave wraps around the cold ashes over the course of the detonation.

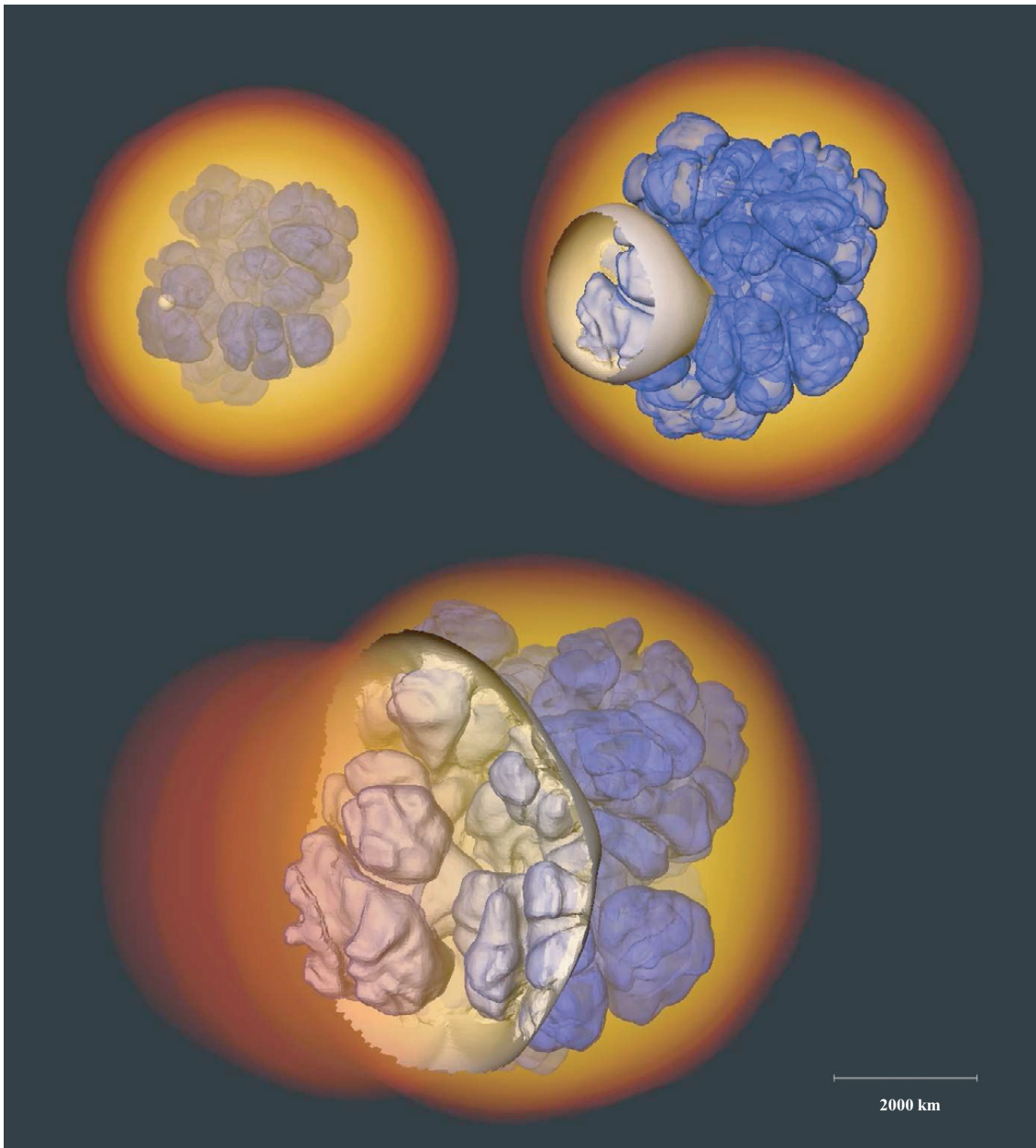


Figure 1.15 Röpke & Bruckschen (2008), (kind permission of Fritz Röpke

An open question is if and how these transitions from deflagration to detonation occur in SNe Ia. This scenario reproduces the light curves and spectra reasonably well (Kasen et al., 2009).

sub-Chandrasekhar-mass detonations The main theme of this explosion mechanism is that a surface detonation drives a shock-wave into the core. In the core this shockwave triggers an ignition by compression. Fink et al. (2010) have explored this scenario theoretically. As an initial model they use a CO-WD accreting from a helium rich companion building a thin helium shell around its CO interior (described in Bildsten et al., 2007). This helium shell is ignited (maybe due to accretion) and sends out a shockwave. As the helium flame spreads on the shell around the star it sends a shockwave into the core. Once the shockwaves converge off-center they create the right environment for the launch of a detonation wave (see Figure 1.16.) The resulting detonation consumes the star. Sim et al. (2010) have simulated the off-center detonation of a sub-Chandrasekhar-mass CO-WD and the resulting light-curve and spectra reproduce observed ones fairly well. This scenario reproduces the intrinsic luminosity variability in the class of SN Ia as each exploding white dwarf can have a different mass. An additional advantage of this model is that it is not in conflict with population synthesis predictions (Ruiter et al., 2009).

WD-WD mergers CO-WD mergers for a long time were thought to lead to a gravitational collapse (same mechanism as the ONe-WD Saio & Nomoto, 1985). Pakmor et al. (2010) has, however, successfully simulated the explosion of two merging CO-WDs. The initial model was two equal mass $0.8 M_{\odot}$ CO-WDs. The merging process created a hotspot from which a detonation wave emanates. The resulting light-curves and spectra are very faint but are similar to sub-luminous SN Ia (e.g. SN 1991bg).

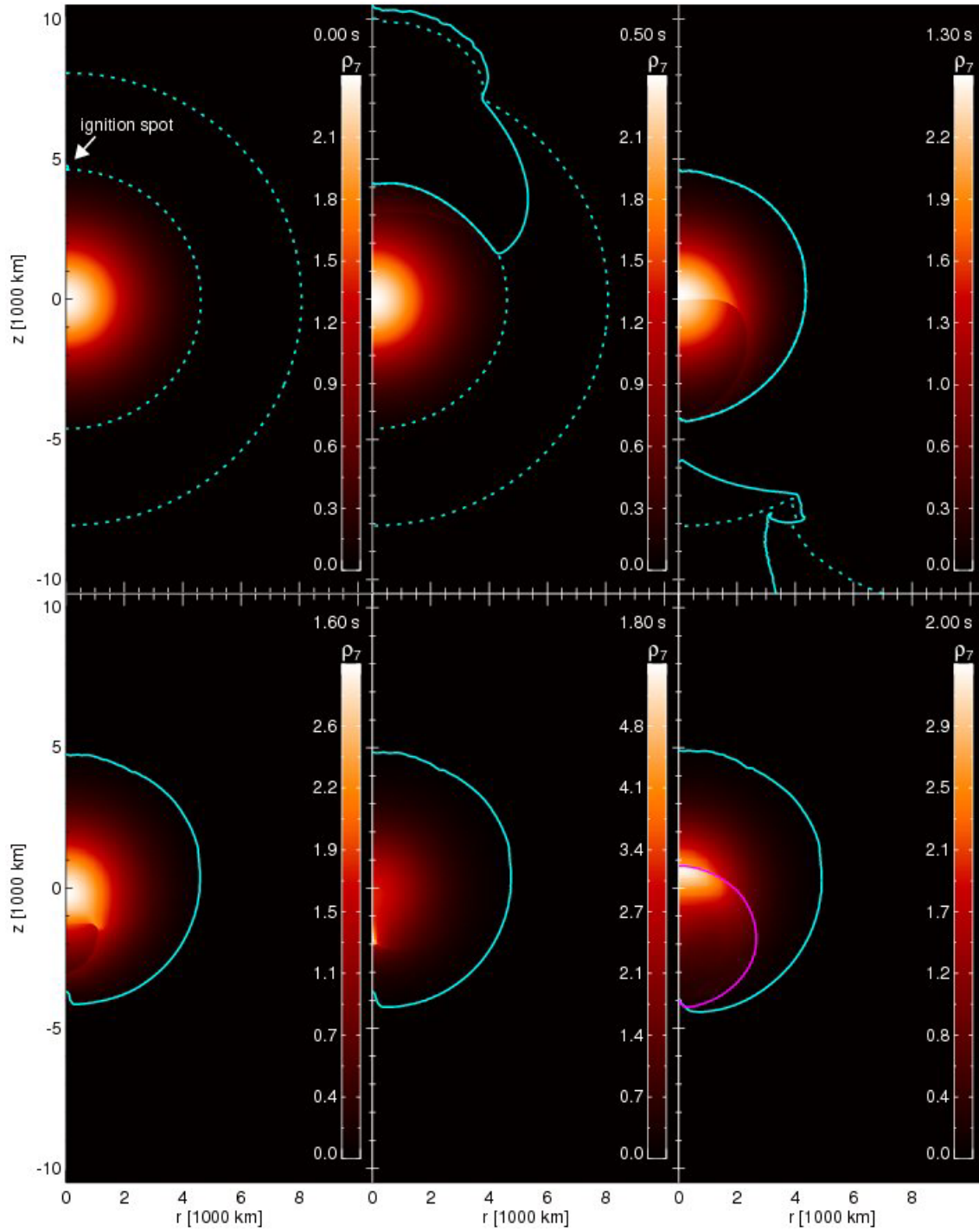


Figure 1.16 example caption

1.6. Progenitors of Type Ia Supernovae

Whelan & Iben (1973) first introduced the modern binary evolution paradigm for SN Ia-progenitors. In their model a CO-WD accreted from a red giant. A degenerate CO-WD accreting from a non-degenerate companion is now known as the single degenerate scenario.

Nomoto & Iben (1985) were one of the first to suggest that the merging of two CO-WDs could also produce SNe Ia. This scenario is now commonly referred to as the double degenerate scenario. Embarrassingly forty years after first progenitor suggestion the progenitors of SN Ia are still not known. Without knowing the precise channel (or channels) for SN Ia it is hard to make precise statements about yields, rates and explosion energies. One of this thesis main goals is finding the remaining companions in ancient SN Ia-remnants (see Chapter ?? and Chapter ??).

1.6.1. Single Degenerate Scenario

In the single degenerate scenario assumes a binary system with one evolved white dwarf and one non-degenerate companion. In most cases this non-degenerate companion is thought to be main-sequence to red giant phase. There are scenario that involve "exotic" companions such as helium stars. The companion (or donor) star is believed to have filled its Roche-Lobe and lose mass via Roche-Lobe-Overflow (RLOF). Different scenarios see accretion from the wind of the companion rather than from RLOF (Mohamed & Podsiadlowski, 2011).

Evolution see mennekens

Accretion The main problem of the SD-scenario is the accretion process. As most white dwarfs are born with masses around $1.6 M_{\odot}$ they need to accrete mass to reach the critical $1.38 M_{\odot}$. The process needs to be efficient as well as burn most accreted hydrogen to explain its lack in the spectrum. If the mass-accretion rate is too low it causes nova explosions which eject are thought to eject more mass than they had accreted prior (Nomoto, 1982). There are however systems (e.g. RS Oph, U Sco) that have white dwarf masses close to $1.4 M_{\odot}$ which have recurrent nova outbursts. It is very likely that these systems weren't born with a white dwarf that massive, but that these white dwarfs accreted all the material. This suggest that despite nova outbursts efficient accretion is possible.

A degenerate layer of helium can form at moderate accretion rates. This layer may flash and could give rise to sub-Chandrasekhar-mass explosions.

A class of binaries called Supersoft X-Ray sources (SSS) probably accrete hydrogen at a high rate. At this rate Hydrogen and Helium burn hydrostatically, if retained, make these objects very strong contenders for SN Ia progenitors. Gilfanov & Bogdán (2010) however have not found enough X-ray flux from elliptical galaxies if all SN Ia-progenitors were these SSS (assuming the X-Ray flux calculated for these objects is correct).

At extremely high accretion rates the white dwarf would be engulfed in an extended red giant envelope. Debris of this envelope is not seen in SN Ia-explosions.

Another subclass of SD-progenitors are AM CVn stars. These type of cataclysmic variable accretes from a helium star. This scenario would very conveniently explain the

lack of hydrogen in SN Ia-explosions. [Fink et al.](#) (see section ?? 2010) have found a way that such systems can explode in a SN Ia.

Donor Stars

The SD-scenario requires a secondary companion (also known as donor) star. If this companion survives the explosion it would be a calling card for the SD-scenario.

[Marietta et al. \(2000\)](#) have simulated the impact of SN Ia-ejecta on main-sequence, sub-giant and red-giant companion. In the case of the main-sequence companion the supernova ejecta heats a small fraction (1-2%) of the envelope which is lost post-explosion. The stellar core cools and expands. It subsequently pulses while going back to hydrostatic equilibrium. [Pakmor et al. \(2008\)](#) have repeated the simulations for the main-sequence companion and find similar results to [Marietta et al. \(2000\)](#). Post-explosion the star could be very luminous ($500 - 5000 L_{\odot}$) due to its asymmetrical temperature distribution. It is expected to cool down between 1400 – 11000 yrs and follow the main-sequence track.

For the sub-giant companion the simulations show very similar results to the main-sequence companion. In summary, the subgiant loses only a small fraction of the envelope (10 – 15%) and will be very luminous shortly after the explosion. After thermal equilibrium is established the companion will return to a post-main-sequence track.

The case of the red-giant, however, is very different. [Marietta et al. \(2000\)](#) suggest that it will lose most of its loosely bound envelope. Post-explosion the remaining core rises contracts and the temperature rises to more than 3×10^4 K. The object may appear as an under luminous main-sequence O or B star.

[Justham et al. \(2009\)](#) have suggested low-mass single white dwarfs to be the remaining cores of red-giant donor stars. This would result in a convenient explanation for the existence of these objects.

One feature of surviving companions may be an unusually large rotational velocity post-explosion ([Kerzendorf et al., 2009](#), chapter ?? of this work). Due to tidal coupling during the RLOF-phase one calculates the expected rotational velocity from the escape velocity of the donor (see Figure ??). Late-type stars usually don't display such high rotational velocities. Thus this feature is a very useful discriminant when looking for donor stars.

Most simulations suggest that the donor-star would survive the explosion one way or another. There have been several attempts to find these objects in ancient supernova remnants. [Schweizer & Middleditch \(1980\)](#) found a OB subdwarf star located 2.5 ' from the center of the remnant of SN1006 and suggested this as the donor star. Subsequent analysis by XXX have however revealed however strong red and blue shifted iron lines. The velocities of these lines are on order of 5000 km s^{-1} which is the same as the velocity of the freely expanding remnant of SN1006.

[Ruiz-Lapuente et al. \(2004\)](#) have suggested a star called Tycho-G by their nomenclature as the progenitor of SN1572. ([Kerzendorf et al., 2009](#); ?, chapter ?? of this work and ??) have followed this up and did not find Tycho-G to be very unusual to the other stars in the field.

citekerz11b have observed 80 stars in the center of SN1006 and have not found an obvious donor star..... ?????

1.6.2. Double Degenerate Scenario

Webbink (1984) was one of the first to suggest merging white dwarfs as progenitors for SN Ia. The one big advantage of the DD-scenario is that it naturally explains the lack of hydrogen in SN Ia-spectra. The accretion problem encountered in the SD-scenario is also alleviated with DD, as long as the sum of masses of both CO-WD's is above M_{Chan} . The work in this thesis has failed to find the companion which may result from the SD-scenario. This would be a further encouragement for the DD-scenario.

The problem, however, is that most SN Ia are relatively homogeneous. It is hard to reconcile this fact with the merger of two white dwarfs with different initial masses, composition, angular momenta and different impact parameters.

Pakmor et al. (2010) have simulated the merger of two equal-mass white dwarfs ($0.8 M_{\odot}$). Their simulations suggest that the outcomes of these mergers would be subluminal. As the star cools after the contraction phase it may become a single Helium white dwarf.

Justham et al. (2009) proposes that In summary, mergers of white dwarfs can definitely explain some of SN Ia. It is however questionable if these events are responsible for the main body of SNe Ia.

1.6.3. Population Synthesis

Population synthesis have been an important step in exploring the different progenitor scenarios. This science is still in its infancy, but results from new all-sky surveys will make this a very precise tool. Ruiter et al. (2009); Mennekens et al. (2010) have explored the SN Ia-rate using different progenitor scenarios (SD, DD and AM CVn). Both suggest that the SD-scenario on its own can not explain the observed supernova rate. The DD-rate seems to be much closer to the observed frequency. Possibly a mix of all channels is required to explain the observed rate.

1.7. Thesis motivation

One of the most pivotal moments in astronomy in recent years was the discovery of the accelerating expanding universe by Riess et al. (1998) and Perlmutter et al. (1999). This discovery catapulted SNe Ia into the limelight of the astronomical community. There has been many advances in recent years in the understanding of these cataclysmic events (explosion models, rates, etc.). One critical piece of the puzzle, however, has so far eluded discovery: The progenitors of SNe Ia. This work's main aim was to find evidence for one SN Ia-progenitor scenario. The SD-scenario proposes a white dwarf accreting from a non-degenerate donor star. To the best of our knowledge this donor star is thought to survive the explosion and would be visible thereafter. We have tried to find this companion in two of three easily accessible ancient supernova remnants (SN1572 and SN1006). In chapter ?? we have obtained spectra of Tycho-G which had been suggested as the donor star of SN1572 (Ruiz-Lapuente et al., 2004). Although we confirmed some of the suggested parameters we could not reproduce the unusually high radial velocity which led to the claim.

We revisited SN1572 in chapter ?? with new observations of Tycho-G and five other stars in the neighbourhood of SN1572. This resulted in Tycho-G to be not a very viable donor star (it is hard to completely rule stars out). We discovered a curious A-Star located

serendipitously right in the center of SN1572. Despite its bizarre parameters we could not reconcile this star (Tycho-B) with any feasible progenitor model. We, however, found a scenario which explains Tycho-B's features but does not involve it in SN1572.

SN1006 provides a perfect opportunity to search for progenitor stars. It is the closest known remnant of a SN Ia (2 kpc). We have obtained 80 spectra of stars close to the center of the remnant and present them in chapter ???. Again we did not find any obvious donor stars.

We have obtained spectra of stars around SN1604 but these are not presented in this work.

Progenitor hunts provide us with information of the scenarios pre-explosion. Spectra on the other hand help to unravel the happenings during and post-explosion. Mazzali et al. ??? have developed a code that can produce synthetic SN Ia-spectra from fundamental input parameters. Fitting an observed SN Ia is for the moment a manual task. This requires many days, if not weeks, of tweaking. The deluge of spectroscopically well-sampled SNe Ia from surveys is already hitting us. Manual analysis of all these spectra is impossible. The information about the explosion hidden in the spectra is, however, crucial to our understanding of these events. In chapter ?? we present our work towards automating this fitting process. We have tried a variety of algorithms to explore the vast and extremely complex search space. Working together with members of the computer science community we are exploring the use of genetic algorithms to solve this problem. This work is not finished yet, but we present preliminary methods in SN Ia-fitting. Once finished we can apply this method not only in fitting SN Ia, but fitting other supernovae and other areas of astronomy.

In summary, this work explores two areas of supernova physics. The hunt for progenitors has not yielded obvious candidates, but may suggest a rethinking of the "normal" SD-scenario. The automation of the supernova fitting is in its infancy stage. We have however shown that it is possible to explore the space in an automated fashion. This will hopefully yield parameters for many thousand supernovae and the next few years. The close collaboration with computer science community has shown how important cross-disciplinary research is in this era of science.

BIBLIOGRAPHY

- Arnett, W. D. 1969, *Ap&SS*, 5, 180
- Baade, W. & Zwicky, F. 1934, *Proceedings of the National Academy of Science*, 20, 254
- Barbon, R., Ciatti, F., & Rosino, L. 1979, *A&A*, 72, 287
- Baron, E., Bethe, H. A., Brown, G. E., Cooperstein, J., & Kahana, S. 1987, *Physical Review Letters*, 59, 736
- Baron, E., Cooperstein, J., & Kahana, S. 1985, *Physical Review Letters*, 55, 126
- Benetti, S., Cappellaro, E., Mazzali, P. A., Turatto, M., Altavilla, G., Bufano, F., Elias-Rosa, N., Kotak, R., Pignata, G., Salvo, M., & Stanishev, V. 2005, *ApJ*, 623, 1011
- Bildsten, L., Shen, K. J., Weinberg, N. N., & Nelemans, G. 2007, *ApJ*, 662, L95
- Brahe, T. & Kepler, J. 1602, *Tychonis Brahe Astronomiae instauratae progymnasmata : quorum haec prima pars de restitutione motuum SOLIS et lunae stellarumque inerrantium tractat, et praeterea de admiranda nova stella anno 1572 exorta luculenter agit.*, ed. Brahe, T. & Kepler, J.
- Chandrasekhar, S. 1931, *ApJ*, 74, 81
- della Valle, M. & Livio, M. 1994, *ApJ*, 423, L31
- Della Valle, M. & Panagia, N. 2003, *ApJ*, 587, L71
- Ensman, L. & Burrows, A. 1992, *ApJ*, 393, 742
- Filippenko, A. V., Li, W. D., Treffers, R. R., & Modjaz, M. 2001, in *Astronomical Society of the Pacific Conference Series*, Vol. 246, IAU Colloq. 183: Small Telescope Astronomy on Global Scales, ed. B. Paczynski, W.-P. Chen, & C. Lemme, 121–+
- Fink, M., Röpke, F. K., Hillebrandt, W., Seitenzahl, I. R., Sim, S. A., & Kromer, M. 2010, *A&A*, 514, A53+

- Garavini, G., Nobili, S., Taubenberger, S., Pastorello, A., Elias-Rosa, N., Stanishev, V., Blanc, G., Benetti, S., Goobar, A., Mazzali, P. A., Sanchez, S. F., Salvo, M., Schmidt, B. P., & Hillebrandt, W. 2007, *A&A*, 471, 527
- Gaskell, C. M., Cappellaro, E., Dinerstein, H. L., Garnett, D. R., Harkness, R. P., & Wheeler, J. C. 1986, *ApJ*, 306, L77
- Gerardy, C. L., Höflich, P., Fesen, R. A., Marion, G. H., Nomoto, K., Quimby, R., Schaefer, B. E., Wang, L., & Wheeler, J. C. 2004, *ApJ*, 607, 391
- Gilfanov, M. & Bogdán, Á. 2010, *Nature*, 463, 924
- Goldstein, B. R. 1965, *AJ*, 70, 105
- Gutiérrez, J., Canal, R., & García-Berro, E. 2005, *A&A*, 435, 231
- Guy, J., Astier, P., Baumont, S., Hardin, D., Pain, R., Regnault, N., Basa, S., Carlberg, R. G., Conley, A., Fabbro, S., Fouchez, D., Hook, I. M., Howell, D. A., Perrett, K., Pritchett, C. J., Rich, J., Sullivan, M., Antilogus, P., Aubourg, E., Bazin, G., Bronder, J., Filiol, M., Palanque-Delabrouille, N., Ripoché, P., & Ruhlmann-Kleider, V. 2007, *A&A*, 466, 11
- Hanbury Brown, R. & Hazard, C. 1952, *Nature*, 170, 364
- Hancock, P., Gaensler, B. M., & Murphy, T. 2011, *ArXiv e-prints*
- Harkness, R. P., Wheeler, J. C., Margon, B., Downes, R. A., Kirshner, R. P., Uomoto, A., Barker, E. S., Cochran, A. L., Dinerstein, H. L., Garnett, D. R., & Levreault, R. M. 1987, *ApJ*, 317, 355
- Hartwig, E. 1885, *Astronomische Nachrichten*, 112, 360
- Hatano, K., Branch, D., Fisher, A., Baron, E., & Filippenko, A. V. 1999, *ApJ*, 525, 881
- Hillebrandt, W. & Niemeyer, J. C. 2000, *ARA&A*, 38, 191
- Hirashita, H., Buat, V., & Inoue, A. K. 2003, *A&A*, 410, 83
- Howell, D. A. 2001, *ApJ*, 554, L193
- Hubble, E. 1929, *Proceedings of the National Academy of Science*, 15, 168
- Hughes, J. P., Chugai, N., Chevalier, R., Lundqvist, P., & Schlegel, E. 2007, *ApJ*, 670, 1260
- Iliadis, C. 2007, *Nuclear Physics of Stars*, ed. Iliadis, C. (Wiley-VCH Verlag)
- Jha, S., Riess, A. G., & Kirshner, R. P. 2007, *ApJ*, 659, 122
- Justham, S., Wolf, C., Podsiadlowski, P., & Han, Z. 2009, *A&A*, 493, 1081
- Kasen, D. 2006, *ApJ*, 649, 939
- Kasen, D., Röpke, F. K., & Woosley, S. E. 2009, *Nature*, 460, 869
- Kepler, J. 1606, *De Stella nova in pede Serpentarii*

- Kepler, S. O., Kleinman, S. J., Nitta, A., Koester, D., Castanheira, B. G., Giovannini, O., Costa, A. F. M., & Althaus, L. 2007, *MNRAS*, 375, 1315
- Kerzendorf, W. E., Schmidt, B. P., Asplund, M., Nomoto, K., Podsiadlowski, P., Frebel, A., Fesen, R. A., & Yong, D. 2009, *ApJ*, 701, 1665
- Kirshner, R. P. & Kwan, J. 1974, *ApJ*, 193, 27
- Klein, R. I. & Chevalier, R. A. 1978, *ApJ*, 223, L109
- Lesaffre, P., Podsiadlowski, P., & Tout, C. A. 2005, *Nuclear Physics A*, 758, 463
- Mannucci, F., Della Valle, M., Panagia, N., Cappellaro, E., Cresci, G., Maiolino, R., Petrosian, A., & Turatto, M. 2005, *A&A*, 433, 807
- Marietta, E., Burrows, A., & Fryxell, B. 2000, *ApJS*, 128, 615
- Mazzali, P. A., Benetti, S., Altavilla, G., Blanc, G., Cappellaro, E., Elias-Rosa, N., Garavini, G., Goobar, A., Harutyunyan, A., Kotak, R., Leibundgut, B., Lundqvist, P., Mattila, S., Mendez, J., Nobili, S., Pain, R., Pastorello, A., Patat, F., Pignata, G., Podsiadlowski, P., Ruiz-Lapuente, P., Salvo, M., Schmidt, B. P., Sollerman, J., Stanishev, V., Stehle, M., Tout, C., Turatto, M., & Hillebrandt, W. 2005, *ApJ*, 623, L37
- Mazzali, P. A., Röpke, F. K., Benetti, S., & Hillebrandt, W. 2007, *Science*, 315, 825
- Meegan, C. A., Fishman, G. J., Wilson, R. B., Horack, J. M., Brock, M. N., Paciesas, W. S., Pendleton, G. N., & Kouveliotou, C. 1992, *Nature*, 355, 143
- Meikle, W. P. S. 2000, *MNRAS*, 314, 782
- Mennekens, N., Vanbeveren, D., De Greve, J. P., & De Donder, E. 2010, *A&A*, 515, A89+
- Minkowski, R. 1941, *PASP*, 53, 224
- Mohamed, S. & Podsiadlowski, P. 2011, in *Asymmetric Planetary Nebulae 5 Conference*
- Nomoto, K. 1982, *ApJ*, 253, 798 [\[LINK\]](#)
- Nomoto, K. & Iben, Jr., I. 1985, *ApJ*, 297, 531
- Nomoto, K. & Kondo, Y. 1991, *ApJ*, 367, L19
- Nugent, P., Phillips, M., Baron, E., Branch, D., & Hauschildt, P. 1995, *ApJ*, 455, L147+
- Nugent, P., Sullivan, M., Ellis, R., Gal-Yam, A., Leonard, D. C., Howell, D. A., Astier, P., Carlberg, R. G., Conley, A., Fabbro, S., Fouchez, D., Neill, J. D., Pain, R., Perrett, K., Pritchett, C. J., & Regnault, N. 2006, *ApJ*, 645, 841
- Pakmor, R., Kromer, M., Röpke, F. K., Sim, S. A., Ruiter, A. J., & Hillebrandt, W. 2010, *Nature*, 463, 61
- Pakmor, R., Röpke, F. K., Weiss, A., & Hillebrandt, W. 2008, *A&A*, 489, 943

- Perlmutter, S., Aldering, G., Goldhaber, G., Knop, R. A., Nugent, P., Castro, P. G., Deustua, S., Fabbro, S., Goobar, A., Groom, D. E., Hook, I. M., Kim, A. G., Kim, M. Y., Lee, J. C., Nunes, N. J., Pain, R., Pennypacker, C. R., Quimby, R., Lidman, C., Ellis, R. S., Irwin, M., McMahon, R. G., Ruiz-Lapuente, P., Walton, N., Schaefer, B., Boyle, B. J., Filippenko, A. V., Matheson, T., Fruchter, A. S., Panagia, N., Newberg, H. J. M., Couch, W. J., & The Supernova Cosmology Project. 1999, *ApJ*, 517, 565
- Phillips, M. M. 1993, *ApJ*, 413, L105
- Phillips, M. M., Wells, L. A., Suntzeff, N. B., Hamuy, M., Leibundgut, B., Kirshner, R. P., & Foltz, C. B. 1992, *AJ*, 103, 1632
- Quimby, R., Höflich, P., Kannappan, S. J., Rykoff, E., Rujopakarn, W., Akerlof, C. W., Gerardy, C. L., & Wheeler, J. C. 2006, *ApJ*, 636, 400
- Riess, A. G., Filippenko, A. V., Challis, P., Clocchiatti, A., Diercks, A., Garnavich, P. M., Gilliland, R. L., Hogan, C. J., Jha, S., Kirshner, R. P., Leibundgut, B., Phillips, M. M., Reiss, D., Schmidt, B. P., Schommer, R. A., Smith, R. C., Spyromilio, J., Stubbs, C., Suntzeff, N. B., & Tonry, J. 1998, *AJ*, 116, 1009
- Riess, A. G., Filippenko, A. V., Li, W., Treffers, R. R., Schmidt, B. P., Qiu, Y., Hu, J., Armstrong, M., Faranda, C., Thouvenot, E., & Buil, C. 1999, *AJ*, 118, 2675
- Riess, A. G., Press, W. H., & Kirshner, R. P. 1995, *ApJ*, 438, L17
- Röpke, F. K. & Bruckschen, R. 2008, *New Journal of Physics*, 10, 125009
- Röpke, F. K. & Hillebrandt, W. 2005, *A&A*, 431, 635
- Ruiter, A. J., Belczynski, K., & Fryer, C. 2009, *ApJ*, 699, 2026
- Ruiz-Lapuente, P., Burkert, A., & Canal, R. 1995, *ApJ*, 447, L69+
- Ruiz-Lapuente, P., Comeron, F., Méndez, J., Canal, R., Smartt, S. J., Filippenko, A. V., Kurucz, R. L., Chornock, R., Foley, R. J., Stanishev, V., & Ibata, R. 2004, *Nature*, 431, 1069
- Saio, H. & Nomoto, K. 1985, *A&A*, 150, L21
- Schlegel, E. M. 1990, *MNRAS*, 244, 269
- Schweizer, F. & Middleditch, J. 1980, *ApJ*, 241, 1039
- Sim, S. A., Röpke, F. K., Hillebrandt, W., Kromer, M., Pakmor, R., Fink, M., Ruiter, A. J., & Seitenzahl, I. R. 2010, *ApJ*, 714, L52
- Soderberg, A. M., Berger, E., Page, K. L., Schady, P., Parrent, J., Pooley, D., Wang, X.-Y., Ofek, E. O., Cucchiara, A., Rau, A., Waxman, E., Simon, J. D., Bock, D. C.-J., Milne, P. A., Page, M. J., Barentine, J. C., Barthelmy, S. D., Beardmore, A. P., Bietenholz, M. F., Brown, P., Burrows, A., Burrows, D. N., Byrnes, G., Cenko, S. B., Chandra, P., Cummings, J. R., Fox, D. B., Gal-Yam, A., Gehrels, N., Immler, S., Kasliwal, M., Kong, A. K. H., Krimm, H. A., Kulkarni, S. R., Maccarone, T. J., Mészáros, P., Nakar, E., O'Brien, P. T., Overzier, R. A., de Pasquale, M., Racusin, J., Rea, N., & York, D. G. 2008, *Nature*, 453, 469

- Soderberg, A. M., Nakar, E., Berger, E., & Kulkarni, S. R. 2006, *ApJ*, 638, 930
- Staelin, D. H. & Reifstein, III, E. C. 1968, *Science*, 162, 1481
- Stehle, M., Mazzali, P. A., Benetti, S., & Hillebrandt, W. 2005, *MNRAS*, 360, 1231
- Tammann, G. A., Loeffler, W., & Schroeder, A. 1994, *ApJS*, 92, 487
- Tanaka, M., Mazzali, P. A., Maeda, K., & Nomoto, K. 2006, *ApJ*, 645, 470
- Tanaka, M., Mazzali, P. A., Stanishev, V., Maurer, I., Kerzendorf, W. E., & Nomoto, K. 2011, *MNRAS*, 410, 1725
- Thomas, R. C., Branch, D., Baron, E., Nomoto, K., Li, W., & Filippenko, A. V. 2004, *ApJ*, 601, 1019
- Turatto, M. 2003, in *Lecture Notes in Physics*, Berlin Springer Verlag, Vol. 598, *Supernovae and Gamma-Ray Bursters*, ed. K. Weiler, 21–36
- Turatto, M., Benetti, S., & Pastorello, A. 2007, in *American Institute of Physics Conference Series*, Vol. 937, *Supernova 1987A: 20 Years After: Supernovae and Gamma-Ray Bursters*, ed. S. Immler, K. Weiler, & R. McCray, 187–197
- van den Bergh, S. & Tammann, G. A. 1991, *ARA&A*, 29, 363
- van Dyk, S. D., Treffers, R. R., Richmond, M. W., Filippenko, A. V., & Paik, Y. 1994, in *Bulletin of the American Astronomical Society*, Vol. 26, *American Astronomical Society Meeting Abstracts*, 1444–+
- Weaver, T. A., Zimmerman, G. B., & Woosley, S. E. 1978, *ApJ*, 225, 1021
- Webbink, R. F. 1984, *ApJ*, 277, 355
- Whelan, J. & Iben, Jr., I. 1973, *ApJ*, 186, 1007
- Wood-Vasey, W. M., Friedman, A. S., Bloom, J. S., Hicken, M., Modjaz, M., Kirshner, R. P., Starr, D. L., Blake, C. H., Falco, E. E., Szentgyorgyi, A. H., Challis, P., Blondin, S., Mandel, K. S., & Rest, A. 2008, *ApJ*, 689, 377
- Woosley, S. E., Heger, A., & Weaver, T. A. 2002, *Reviews of Modern Physics*, 74, 1015
- Zhao, F., Strom, R. G., & Jiang, S. 2006, *Chinese J. Astron. Astrophys.*, 6, 635
- Zwicky, F. 1938, *ApJ*, 88, 529